

Qualitative Analysis of Optic Nerve Head Peripapillary  
Microvasculature in Healthy Eyes Using Optical Coherence  
Tomography Angiography

Mr. Sittikorn Laojaroenwanit



A Thesis Submitted in Partial Fulfillment of the Requirements  
for the Degree of Master of Science in Clinical Sciences  
Common Course  
FACULTY OF MEDICINE  
Chulalongkorn University  
Academic Year 2019  
Copyright of Chulalongkorn University

การตรวจวิเคราะห์เชิงคุณภาพเส้นเลือดรอบขั้วประสาทตาในกลุ่มคนทั่วไปโดยใช้เครื่องตรวจ  
วิเคราะห์เส้นเลือดขั้วประสาทตาด้วยเลเซอร์



วิทยานิพนธ์นี้เป็นส่วนหนึ่งของการศึกษาตามหลักสูตรปริญญาวิทยาศาสตรมหาบัณฑิต  
สาขาวิชาเวชศาสตร์คลินิก ไม่สังกัดภาควิชา/เทียบเท่า  
คณะแพทยศาสตร์ จุฬาลงกรณ์มหาวิทยาลัย  
ปีการศึกษา 2562  
ลิขสิทธิ์ของจุฬาลงกรณ์มหาวิทยาลัย

|                   |  |
|-------------------|--|
| Thesis Title      | Qualitative Analysis of Optic Nerve Head Peripapillary<br>Microvasculature in Healthy Eyes Using Optical<br>Coherence Tomography Angiography |
| By                | Mr. Sittikorn Laojaroenwanit   |
| Field of Study    | Clinical Sciences  |
| Thesis Advisor    | KITTISAK KULVICHIT   |
| Thesis Co Advisor | ADISAI VARADISAI   |

---

Accepted by the FACULTY OF MEDICINE, Chulalongkorn University in  
Partial Fulfillment of the Requirement for the Master of Science

..... Dean of the FACULTY OF  
MEDICINE  
(SUTTIPONG WACHARASINDHU)

THESIS COMMITTEE

..... Chairman  
(PRASART LAKSANAPHUK)  
..... Thesis Advisor  
(KITTISAK KULVICHIT)  
..... Thesis Co-Advisor  
(ADISAI VARADISAI)  
..... Examiner  
(THANAPONG SOMKIJRUNGROJ)  
..... External Examiner  
(SRITATATH VONGKULSIRI)

จุฬาลงกรณ์มหาวิทยาลัย  
CHULALONGKORN UNIVERSITY

สิทธิกรณธ์ เจ้าเจริญวานิชย์ : การตรวจวิเคราะห์เชิงคุณภาพเส้นเลือดรอบหัวประสาทตาในกลุ่มคนทั่วไปโดยใช้เครื่องตรวจวิเคราะห์เส้นเลือดหัวประสาทตาด้วยเลเซอร์. ( Qualitative Analysis of Optic Nerve Head Peripapillary Microvasculature in Healthy Eyes Using Optical Coherence Tomography Angiography) อ.  
 ที่ปรึกษาหลัก : กิตติศักดิ์ กุลวิจิตร, อ.ที่ปรึกษาร่วม : อติษฐ์ วราดิษฐ์

วัตถุประสงค์หลัก: เพื่อศึกษาเส้นเลือดรอบหัวประสาทตาในกลุ่มคนทั่วไปโดยใช้เครื่องตรวจวิเคราะห์เส้นเลือดด้วยเลเซอร์

วัตถุประสงค์รอง: เพื่อศึกษาเส้นเลือดจอประสาทตาบริเวณจุดรับภาพชัดในกลุ่มคนทั่วไปโดยใช้เครื่องตรวจวิเคราะห์เส้นเลือดด้วยเลเซอร์

รูปแบบงานวิจัย: การศึกษาแบบตัดขวาง

ผู้เข้าร่วมงานวิจัย: 224 คน จากอาสาสมัคร 112 คน ที่มีสุขภาพสมบูรณ์ที่โรงพยาบาลจุฬาลงกรณ์

วิธีการศึกษา: อาสาสมัครเข้ารับการถ่ายภาพจอประสาทตาและเส้นเลือดที่จอประสาทตา โดยภาพถ่ายตรงหน้าขนาด 3x3 มิลลิเมตรบริเวณจุดรับภาพชัด ภาพถ่ายตรงหน้าขนาด 6x6 มิลลิเมตรบริเวณหัวประสาทตา ภาพถ่ายตัดขวางตัดผ่านจุดรับภาพชัดและหัวประสาทตาขนาด 16 มิลลิเมตร โดยเครื่องตรวจวิเคราะห์เส้นเลือดด้วยเลเซอร์

ผลการศึกษา: ความหนาแน่นของเส้นเลือดรอบหัวประสาทตาหนาแน่นมากที่สุดบริเวณด้านล่างส่วนนอกของหัวประสาทตา โดยมีค่าความหนาแน่นเฉลี่ย±ส่วนเบี่ยงเบนมาตรฐานเท่ากับ  $17.99 \pm 2.00$  ตารางมิลลิเมตร ความหนาแน่นของเส้นเลือดรอบหัวประสาทตาหนาแน่นน้อยที่สุดบริเวณด้านในของหัวประสาทตา โดยมีค่าความหนาแน่นเฉลี่ย±ส่วนเบี่ยงเบนมาตรฐานเท่ากับ  $14.20 \pm 1.82$  ตารางมิลลิเมตร ขนาดพื้นที่บริเวณที่ไม่มีเลือดไหลเวียนบริเวณจุดรับภาพชัดชั้นผิวมีขนาดเฉลี่ย±ส่วนเบี่ยงเบนมาตรฐานเท่ากับ  $0.31 \pm 0.1$  ตารางมิลลิเมตร ส่วนขนาดพื้นที่บริเวณที่ไม่มีเลือดไหลเวียนบริเวณจุดรับภาพชัดชั้นลึกมีขนาดเฉลี่ย±ส่วนเบี่ยงเบนมาตรฐานเท่ากับ  $0.56 \pm 0.22$  ตารางมิลลิเมตร

สรุปผลการศึกษา: การศึกษานี้ให้ค่ามาตรฐานของความหนาแน่นของเส้นเลือดฝอยรอบหัวประสาทตา และขนาดพื้นที่บริเวณที่ไม่มีเลือดไหลเวียนบริเวณจุดรับภาพชัดในคนไทยโดยการใช้เครื่องตรวจวิเคราะห์เส้นเลือดด้วยเลเซอร์ โดยค่ามาตรฐานนี้สามารถนำไปประยุกต์ใช้เพื่อตรวจวินิจฉัย หรือติดตามการรักษาในกลุ่มภาวะผิดปกติของเส้นเลือดบริเวณจอประสาทตาได้

จุฬาลงกรณ์มหาวิทยาลัย  
 CHULALONGKORN UNIVERSITY

สาขาวิชา เวชศาสตร์คลินิก  
 ปีการศึกษา 2562

ลายมือชื่อ นิสิต .....  
 ลายมือชื่อ อ.ที่ปรึกษาหลัก .....  
 ลายมือชื่อ อ.ที่ปรึกษาร่วม .....

# # 5974654930 : MAJOR CLINICAL SCIENCES

KEYWORD: peripapillary microvasculature, radial peripapillary capillary, optic nerve head microvasculature, macular microvasculature, macular microvascular network, Swept-source optical coherence tomography angiography

Sittikorn Laojaroenwanit : Qualitative Analysis of Optic Nerve Head Peripapillary Microvasculature in Healthy Eyes Using Optical Coherence Tomography Angiography.

Advisor: KITTISAK KULVICHIT Co-advisor: ADISAI VARADISAI

Primary objective: To evaluate optic nerve head microvasculature/radial peripapillary capillaries (RPCs) in healthy adult eyes using swept-source optical coherence tomography angiography

Secondary objectives: To evaluate macular microvascular network in healthy adult eyes using swept-source optical coherence tomography angiography

Design: Cross-sectional study

Participants: 224 eyes of 112 healthy adult volunteers at eye clinic of King Chulalongkorn Memorial Hospital.

Method: En face 3x3-mm OCTA at macular area, 6x6-mm OCTA at optic nerve head and high-definition horizontal lines 16-mm scans crossing the fovea and optic disc were acquired using the SS-OCTA Plex Elite 9000. To evaluate RPCs density, the images were binarized and skeletonized. En face 3x3-mm image used to evaluate both of superficial capillaries and deep capillaries foveal avascular zone(SCP-FAZ and DCP-FAZ)

Main Outcome and Measures: The radial peripapillary capillaries vessel density

Result: The RPCs vessel density was the most crowded at inferotemporal quadrant in all age groups with mean±SD vessel density of 17.99±2.00. The lightest quadrant was nasal quadrant with mean±SD vessel density of 14.20±1.82. The mean±SD of SCP-FAZ and DCP-FAZ were 0.31 ±0.1 mm<sup>2</sup>, 0.56 ±0.22 mm<sup>2</sup> respectively.

Conclusion: Our study gives the SS-OCT/OCTA normative database using the PLEX Elite 9000 device of RPCs density, FAZ area in healthy eyes of Thai people. This baseline database of healthy eyes may used to help for detect, early diagnosis or monitor in the pathologic eyes. Further investigation in pathologic eye is needed.

Field of Study: Clinical Sciences  
Academic Year: 2019

Student's Signature .....  
Advisor's Signature .....  
Co-advisor's Signature .....

## ACKNOWLEDGEMENTS

I would like to express my deep sense of gratitude to my major advisor, Dr. Kittisak Kulvichit for his valuable guidance, suggestion, encouragement and constructive feedback. I am very grateful to my co-advisors Dr. Adisai Varadisai for his knowledge and assistance in this study and Dr. Thanapong Somkitrunroj for being an outstanding mentor, guider and facilitator. I am immensely grateful for their constant guidance, suggestions and support. I would like to thank Dr. Pear Pongsacharoennont and all staff of Retina Research Unit for your confidence in me and for all of your support in this study.

Last but not least, I would like to express immeasurable appreciation and deepest gratitude to my family and colleagues for their enduring support, valuable encouragement, and understanding throughout my study.

Sittikorn Laojaroenwanit



## TABLE OF CONTENTS

|   | <b>Page</b> |
|---|-------------|
| .....   | iii         |
| ABSTRACT (THAI).....                                    | iii         |
| .....   | iv          |
| ABSTRACT (ENGLISH).....                                 | iv          |
| ACKNOWLEDGEMENTS .....                                  | v           |
| <b>TABLE OF CONTENTS</b> .....                          | <b>vi</b>   |
| <b>LIST OF TABLES</b> .....                             | <b>ix</b>   |
| <b>LIST OF FIGURES</b> .....                            | <b>x</b>    |
| <b>CHAPTER I</b> .....                                  | <b>11</b>   |
| <b>INTRODUCTION</b> .....                               | <b>11</b>   |
| 1.1 Rationale.....                                      | 11          |
| 1.2 Objectives.....                                     | 16          |
| 1.3 Research question.....                              | 16          |
| 1.4 Hypothesis.....                                     | 16          |
| 1.5 Variable.....                                       | 17          |
| 1.6 Definitions.....                                    | 17          |
| 1.7 Scope of Study.....                                 | 17          |
| 1.8 Expected or anticipated benefit gain.....           | 18          |
| <b>CHAPTER II</b> .....                                 | <b>19</b>   |
| <b>REVIEW OF RELATED LITERATURE AND RESEARCH</b> ... 19 |             |
| 2.1 Radial peripapillary capillaries plexus.....        | 19          |

|  |    |
|--|----|
| 2.2 Foveal avascular area .....  | 20 |
| 2.3 Posterior vitreous degeneration (PVD) .....                              | 21 |
| CHAPTER III .....  | 22 |
| RESEARCH METHODOLOGY .....   | 22 |
| 3.1 Target population.....   | 22 |
| 3.2 Sample size.....   | 22 |
| 3.3 Approach to participant.....   | 23 |
| 3.4 Research instrument.....   | 24 |
| 3.5 Research processing.....   | 24 |
| 3.6 Data analysis and statistics.....  | 27 |
| 3.7 Ethical considerations.....  | 28 |
| 3.8 Risk and investigation responsibility.....                               | 30 |
| CHAPTER IV .....   | 31 |
| RESULTS .....  | 31 |
| 4.1 Radial Peripapillary Capillaries vascular density.....                   | 31 |
| 4.2 Foveal Avascular Zone (FAZ) and Foveal Macular<br>Thickness (FMT).....   | 32 |
| 4.3 Posterior Vitreous Detachment (PVD).....                                 | 34 |
| CHAPTER V .....  | 36 |
| DISCUSSION, CONCLUSION AND SUGGESTIONS .....                                 | 36 |
| 5.1 Discussion.....  | 36 |
| 5.1.1 Radial Peripapillary Capillaries vascular density .....                | 36 |
| 5.1.2 Foveal Avascular Zone (FAZ) and Foveal Macular<br>Thickness (FMT)..... | 37 |



|   |    |
|---|----|
| 5.1.3 Posterior Vitreous Detachment (PVD).....                                | 40 |
| 5.2 Conclusion.....   | 42 |
| 5.2.1 Radial Peripapillary Capillaries vascular density .....                 | 42 |
| 5.2.2 Foveal Avascular Zone (FAZ) and Foveal Macular<br>Thickness (FMT) ..... | 42 |
| 5.2.3 Posterior Vitreous Detachment (PVD) .....                               | 43 |
| 5.3 The strengths of this study.....  | 43 |
| 5.4 The limitation of this study.....   | 43 |
| 5.5 Suggestion.....   | 44 |
| REFERENCES .....  | 5  |
| VITA.....   | 14 |

## LIST OF TABLES

|   | <b>Page</b> |
|---|-------------|
| Table 1 Baseline demographic data of the 112 subjects.....                                  | 52          |
| Table 2 Vascular density between Rt and Lt eye .....  | 53          |
| Table 3 Normative data of vascular density .....  | 54          |
| Table 4 Mean foveal avascular zone and foveal macular thickness according to eye side ..... | 55          |
| Table 5 FAZ and FMT in different age groups.....  | 56          |
| Table 6 Univariate and Multivariate analysis of SCP-FAZ.....                                | 57          |
| Table 7 Univariate and Multivariate analysis of DCP-FAZ.....                                | 58          |
| Table 8 Univariate and Multivariate analysis of FMT .....                                   | 59          |
| Table 9 Correlation between vitreous structure and age groups.                              | 60          |
| Table 10 FAZ area measured by OCTA of healthy eyes in different studies .....               | 1           |

## LIST OF FIGURES

|  | <b>Page</b> |
|--|-------------|
| Figure 1 Acquisition image .....   | 45          |
| Figure 2 Quadrant of RPCs .....  | 45          |
| Figure 3 An OCTA maps 3*3 mm macular area (A–SCP, B–DCP).....  | 46          |
| Figure 4 A linear 16 mm high-definition B-scan centered on the fovea for foveal macular thickness evaluation .....           | 46          |
| Figure 5 The SS-OCT imaging used for PVD evaluation .....  | 47          |
| Figure 6 Stage of PVD Development.....   | 48          |
| Figure 7 Grading of vitreous degeneration .....  | 50          |
| Figure 8 Box plot of vascular density between Rt and Lt eye .....  | 55          |
| Figure 9 Bar chart showing a comparison of the distribution of the vitreous degeneration grading among the 3 age groups..... | 61          |

## CHAPTER I

### INTRODUCTION

#### 1.1 Rationale

The Human senses are the contact to the environment. Human have five senses: to see, to taste, to smell, to hear and to touch. The eye is the organ to see, Seeing is the most import sense of humankind. How we are seeing, when the light hits the object and reflects into the eyes. The light enters the eyes through the black spot in the middle called the pupil. The pupil can change size by the iris. After that the light pass through to vitreous and focus on the retina.

The vitreous is a gelatinous material that fills intra-ocular space(1, 2). Vitreous composed of water, collagen, and hyaluronic acid. The vitreous body is divided into 2 main topographic areas: the central or core and the peripheral or cortical vitreous(3). The anterior surface of the vitreous body is called the anterior cortical gel forming the ligament of the Wieger. The posterior attachment of the vitreous to the macula forms a space known as the bursa premacularis or the precortical posterior vitreous pocket (PPVP)(4, 5). Anomalous posterior vitreous detachment (PVD) is associated with pathologic conditions, such as macular hole, vitreomacular traction syndrome, or epiretinal membrane(6, 7).

The retina is the innermost, light-sensitive layer of tissue of the eye. Center of the retina called macula, measure 5.5 mm in diameter and located between the optic disc and the temporal vascular arcades. The center 1.5 mm of the macula is called the fovea, which is specialized for high spatial acuity and for color vision. The fovea has a margin, declivity, and floor known as the foveola, 0.35 mm diameter where cones

are slender, elongated and densely packed. The umbo, a small depression 150 – 200  $\mu\text{m}$ , is the center of the foveola. Within the fovea is a region devoid of vessels known as the foveal avascular zone (FAZ). FAZ is an important landmark in fluorescein angiography. FAZ is a highly specialized region of the human retina for the accurate vision(8). The change of FAZ causing the impair of the vision(9, 10).

Retina is stratified into ten distinct layers. From closest to farthest from the vitreous:

- I. Internal limiting membrane - basement membrane is formed by footplate of Muller cells.
- II. Nerve fiber layer – axon of the ganglion cell nuclei.
- III. Ganglion cell layer – contains nuclei of ganglion cells.
- IV. Inner plexiform layer – contains the synapse between the bipolar cell axons and the dendrites of the ganglion and amacrine cells.
- V. Inner nuclear layer – contains the cell bodies of amacrine cells, bipolar cells, and horizontal cells.
- VI. Outer plexiform layer – contains of the synapse between rods/cones ending with dendrites of bipolar cells/horizontal cells. In the macular region, this is known as the Henle's fiber layer.
- VII. Outer nuclear layer – contains of cell body of rods and cones.
- VIII. External limiting membrane – a network-like structure that separates the inner segment portions of the photoreceptors from cell nuclei.
- IX. Photoreceptor layer – contains inner segment and outer segment of rods and cones.

- X. Retinal pigment epithelium – single layer of cuboidal cells. This layer is closest to choroid.

Optic Nerve Head (ONH) is the point of exit for ganglion cell axon leaving the eye to connect primarily to the lateral geniculate body.

Retina circulation supplies by ophthalmic artery. The ophthalmic artery bifurcates and supplies retina via two vascular networks, the choroidal network, which supplies choroid and outer retina, and the retinal network, which supplies inner retina. The retinal network from the central retinal artery divided into superior and inferior branches and then divided into nasal and temporal branches. All the major vessels are in the nerve fiber layer. The arterioles send precapillary branches to the three capillaries layers, the superficial capillaries plexus, intermediate capillaries plexus and deep capillaries plexus. Whereas ONH is mainly supplies by posterior ciliary artery (PCAs) via the peripapillary choroid and short PCAs (or the circle of Zinn and Haller) (11, 12). In addition, another dense layer of capillaries around the optic disc at the posterior pole has been described, which called the layer of radial peripapillary capillaries (RPCs).

The RPCs in the human retina were first described by Michaelson (13) in 1954 as a unique plexus of capillary bed, which are limited in distribution to the posterior pole and seem to be oriented parallel to the retinal nerve fiber layer. RPCs have received but scant attention in the past. Henkind (14) studied in Indian ink-injected retinae of man, rhesus monkey, cat, and pig. Henkind noted that in human retina RPCs were particularly dense aggregation of small vessels surrounding the optic nerve head and most prominent immediately around the disc and in the inferotemporal and superotemporal quadrant. This layer of vessels lied superficial to

the other retinal capillaries and run parallel along extend outwards from the optic disc. RPCs rarely anastomosed with each other, and after running along superficially for a variable distance, RPCs appeared to enter the deeper retina.

Due to the presence of RPCs appears to be intimately tied to the highly metabolically active retinal ganglion cell axon(14), the function of RPCs is most likely to nourish the inner portion of retinal nerve fiber layer (RNFL). According to the unique pattern and distribution of the RPCs resemble the pattern of Bjerrum scotoma, so it was thought that RPCs might be more vulnerable to increase in the intraocular pressure (IOP) than other retinal capillaries and may play a role in the pathogenesis of glaucomatous visual field defect.

In the past, studies of RPCs were limited by lack of image modality. The RPCs were described from histologic analysis by Michaelson in 1954(13). Henkind(14) published article about the RPCs based on India ink-injected eye in 1967-1968. Fluorescein Angiography (FA) was adopted by early pioneers in medical retina research for studying the retinal vasculature and become the standard criterion for in vivo evaluation of the retinal circulation, however the RPCs do not appear to be image well. Adaptive optics scanning light ophthalmoscopy (AOSLO) equipped with FA or a non-confocal detection scheme has had the most success with imaging the RPCs in vivo(15). However, this technique was time-consuming and not clinically optimized.

Optical Coherence Tomography (OCT) is a non-invasive, non-contact imaging modality that produces micrometer-resolution cross-sectional images. OCT working is based on imaging reflected light. The technique produces a 2-dimensional image of the backscattered light from different layers. From the beginning, OCT image were

acquired in a time-domain (TD) fashion. Time-domain OCT(TD-OCT) systems acquire approximately 400 A-scan per second using 6 radial slices orientate 30 degree apart(16). Spectral domain OCT (SD-OCT) scan approximately 20,000 – 40,000 A-scans per second. The increased scan rate diminishes the motion artifact, enhances the resolution and decreases the chance of missing lesions. Currently, SD-OCT is widely used over the earlier TD-OCT(17). Swept-source (SS)-OCT is the latest milestone in OCT technology with a tunable laser operating using a longer-wavelength light source, 1050 nm, and a high-speed photodetector instead of a spectrometer. The scan speed in SS-OCT is twice than SD-OCT (100,000 A-scans per second compare with 50,000 A-scans per second). SS-OCT provides better resolution and increasing depth of retinal image.

OCT was one of the biggest advanced in ophthalmic imaging. Building on that platform, Optical Coherence Tomography Angiography (OCTA) provides depth resolved images of blood flow in the retina and choroid. OCTA is a novel technology. OCTA can produce images of blood flow that have unprecedented resolution of all the vascular layers of the retina in a rapid, non-invasive fashion. While image from FA obscured the deep of retinal blood vessels making only the superficial vascular plexus can be seen. OCTA can imaging the radial peripapillary capillary network and the intermediate and deep capillary plexuses(18).

This study aims to describe the variables of RPCs in normal human retina using OCTA image and proposes a method to measure capillary density of RPCs around ONH.



## 1.2 Objectives

### 1.2.1 Primary Objectives

- To evaluate ONH microvasculature in healthy adult eyes using SS-OCTA

### 1.2.2 Secondary Objective

- To evaluate macular microvascular network in healthy adult eyes using SS-OCTA
- To evaluate foveal macular thickness in healthy adult eyes using SS-OCT
- To evaluate posterior vitreous detachment classification in healthy adult eyes using wide field SS-OCT

## 1.3 Research question

What is the quantitative analysis of ONH microvasculature in healthy adult eyes when using SS-OCTA ?

## 1.4 Hypothesis

Normative data of quantitative analysis of ONH microvasculature in healthy adult eyes in King Chulalongkorn Memorial Hospital are not difference when compare to other previous study.

## 1.5 Variable

**1.5.1 Independent variables:** RPCs vessel density, FAZ at superficial capillaries plexus (SCP) and deep capillaries plexus (DCP), foveal macular thickness (FMT)

**1.5.2 Dependent variables:** Age, gender, smoking status, alcohol drinking status, refractive error

## 1.6 Definitions

**1.6.1 Radial peripapillary capillaries density** was defined as a measurement of unique vascular plexus in the retinal nerve fiber layer from optic nerve head 3 mm.

**1.6.2 Foveal avascular zone** was defined as a region devoid of retinal blood vessels within the fovea.

**1.6.3 Foveal macular thickness** was defined as the layers of the retina and determines macular thickness by measuring the distance between internal limiting membrane and the inner boundary of retinal pigment epithelium.

## 1.7 Scope of Study

A cross sectional study of healthy adult volunteers at King Chulalongkorn Memories Hospital was done. The quantitative analysis of ONH microvasculature in healthy adult eyes using SS-OCTA was described.

## **1.8 Expected or anticipated benefit gain**

**1.8.1** Result of the study can be further applied as reference for normative data of density of RPCs of Thai people.

**1.8.2** Result of the study can be further applied as reference for normative data of FAZ of Thai people.



## CHAPTER II

### REVIEW OF RELATED LITERATURE AND RESEARCH

#### 2.1 Radial peripapillary capillaries plexus

Axons or nerve fibers typically conduct electrical impulses known as action potentials away from the nerve cell body. There are two types of nerve fibers: myelinated and unmyelinated nerve fibers. The nerve fibers in the retina are unmyelinated. Nerve fibers need large amounts of nutrients and oxygen supply to maintain their function. The RPCs supply oxygen and essential metabolites to the nerve fiber. Previous studies of the RPCs plexus had a limitation due to the abilities of image modality. Up to the time of OCTA era, capillary circulation of the ONH and the peripapillary region are well-seen.

In 2012, Jia et al. reported a reduction of vessels density and flow index of RPCs plexus in pre-perimetric glaucoma patients compared to normal eyes(19). Leveque et al found a similar result, 20-25% reduction in ONH vessels density in a cohort of glaucomatous eyes compared to normal eyes(20). Many studies reported the difference of vessels density between normal healthy eyes and glaucomatous eyes. Chen et al. found that the ONH vessels density reduction also correlated with visual field and structural OCT findings(21).

Not only in glaucoma spectrum, OCTA has also been used to evaluate other optic nerve and central nervous system disorders. In patients with multiple sclerosis, Wang and colleagues reported the significant loss of the RPCs plexus in optic neuritis. In optic atrophy, the loss of capillaries in the region affected by the injury was found in many studies.

## 2.2 Foveal avascular area

Macula is an oval shaped pigmented area near the center of the retina. The macula subdivided into the umbo, foveola, parafoveal and perifoveal. The macula function is responsible to the center, high-resolution, and color vision. Foveal microvascular network is affected in many retinal diseases. FAZ is a highly specialized region of the human retina for the accurate vision(8). Many imaging modalities focus in FAZ shape and size in normal eyes. The change of FAZ causing the impair of the vision(9, 10).

The gold standard for mapping retinal vasculature is FA. FA was used to study of ocular vascular system abnormalities and the FAZ in many retinal vascular diseases. Recently, OCTA is a novel non-invasive imaging modality, allowing en face visualization of the retina and separately of both superficial (SCP) and deep retinal capillaries plexuses (DCP) (22, 23). Wylegala et al.(24) created a study to measure and compare the retinal vascular parameter and FAZ in Chinese and Caucasian population. The result shown the Chinese population had larger FAZ than the Caucasian population (FAZ size  $0.33 \pm 0.012 \mu\text{m}$  versus  $0.28 \pm 0.014 \mu\text{m}$  respectively). Falavarjani et al (25) enrolled 70 healthy subjects to report the normal characteristics and correlations of the foveal microvascular networks using OCTA. The study found that mean FAZ area was  $0.32 \pm 0.11 \text{ mm}^2$  in SCP and  $0.50 \pm 0.13 \text{ mm}^2$  in DCP and central foveal subfield thickness was a major determinant of the FAZ size. Previous studies have reported major variation in FAZ area in healthy eye(15, 26, 27). Fujiwara et al. reported that central retinal thickness and retinal vascular density were inversely correlated with FAZ area in healthy eyes.(28)

### 2.3 Posterior vitreous degeneration (PVD)

The vitreous is a gelatinous material that fills intra-ocular space.(1, 2) Vitreous composed of water, collagen, and hyaluronic acid. The vitreous body is divided into 2 main topographic areas: the central or core and the peripheral or cortical vitreous(3). The anterior surface of the vitreous body is called the anterior cortical gel forming the ligament of the Wieger. The posterior attachment of the vitreous to the macula forms a space known as the bursa premacularis or the precortical vitreous pocket (PPVP)(4, 5). In the past, study of vitreous structure had limitation because of the properties of transparent, fluid, and fragile of the vitreous. Most of information is based on post-mortem pathologic studies(1). With the advancement of OCT fashion, SD-OCT in vivo imaging of the posterior vitreous can be imaged. Kim et al. reported the noninvasive imaging of posterior vitreous structures, such as area of Martegiani and bursa premacularis by using SD-OCT(29). After SS-OCT debut, high-quality vitreous images can be obtained due to SS-OCT's longer wavelength and software enhancement(4, 30). Itakura et al. reported bursa premacularis in healthy adults had a mean height and width of 708.1  $\mu\text{m}$  and 6,420.6  $\mu\text{m}$ , respectively(30). And found that bursa premacularis central height increased with myopic refractive errors. Ninety-three percent of eyes had the connection between bursa premacularis and Cloquet's canal. Park et al. reported bursa premacularis detection rate was 91.5% in eyes without PVD, 21% in eyes with partial PVD, and 0% in eyes with complete PVD(31). The bursa premacularis is boat-shaped in horizontal line scan(4), and vertical-oval and round shape in en face image(31).

## CHAPTER III

### RESEARCH METHODOLOGY

The cross-sectional descriptive study was conducted. The main purposes of this study were to evaluate ONH microvasculature in healthy adult eyes using SS-OCTA. This study was approved by the Institutional Reviews Board of Faculty of Medicine, Chulalongkorn University. (IRB No.492/60)

#### 3.1 Target population

Healthy adult volunteers at eye clinic of King Chulalongkorn Memorial Hospital were enrolled in this study.

#### 3.2 Sample size

The participants of this cross-sectional study were calculate from the formula

$$N = [(Z\alpha/2)(\delta)/E]^2$$

$$\delta = 1.4$$

$$E = 0.2$$

$$N = 188 \text{ eyes}$$

##### 3.2.1 Inclusion Criteria

- BCVA score  $\geq 20/70$
- Refractive error from -3.0 to +3.0 D of spherical equivalent
- Intraocular pressure  $\leq 21$  mmHg
- Normal eye fundus
- Normal macular OCT

### 3.2.2 Exclusion criteria

- Previous or current history of ophthalmic diseases related to posterior segment
- Any previous intraocular treatment (such as intra-vitreous injection of anti-VEGF/steroid or retinal LASER)
- Any previous intraocular surgery (such as cataract surgery or retinal surgery)
- Neurodegenerative diseases (such as Parkinson's disease, Alzheimer's disease)
- Any systemic disease with ocular involvement
- Poor collaboration of complete ophthalmic examination
- Poor quality of OCT/OCTA image due to significant opaque media or poor subjects' cooperation

### 3.3 Approach to participant

Informed consent was obtained from all subjects prior to enrollment in the study. The subjects' demographic data including age, sex, best corrected visual acuity (BCVA), results of autorefractometry measurements, air-puff tonometry, smoking status, and alcohol drinking status were recorded.

Each subject underwent a complete ophthalmologic examination including best corrected visual acuity determination using the standard Early Treatment Diabetic Retinopathy Study (EDTRS) chart at 4 meters distance, intraocular pressure measurement by air-puff tonometer and confirmed by Goldmann tonometer in subjects who air-puff greater than 21 mmHg, Slit-lamp dilated fundus examination



with 90D lens, and acquisition of color fundus photography of the posterior pole. SS-OCT and SS-OCTA images were acquired with PLEX Elite 9000 (Carl Zeiss Meditec Inc., Dublin, California, USA)

### **3.4 Research instrument**

- Case record form
- EDTRS chart
- Autorefractometer
- Air-puff tonometer
- Slit lamp microscope
- SS-OCTA

### **3.5 Research processing**

#### **3.5.1 Data collection process**

A cross-sectional study was conducted at King Chulalongkorn Memorial Hospital, Bangkok, Thailand. Data collection was done after the Institutional Reviews Board of Chulalongkorn University, Faculty of Medicine approved the study (IRB No.492/60). Healthy volunteers were prospectively recruited by announcement at the hospital. Informed consent was obtained from all subjects prior to enrollment in the study. The subjects' demographic data including age, sex, BCVA, results of autorefraction measurements, air-puff tonometry, smoking status, and alcohol drinking status were recorded.

Each subject underwent a complete ophthalmologic examination including best correct visual acuity determination using the standard EDTRS chart at 4 meters distance, intraocular pressure measurement by air-puff tonometer and confirmed by

Goldmann tonometer in subjects who air-puff greater than 21 mmHg, Slit-lamp dilated fundus examination with 90D lens, and acquisition of color fundus photography of the posterior pole. SS-OCT and SS-OCTA images were acquired with PLEX Elite 9000 (Carl Zeiss Meditec Inc., Dublin, California, USA)

Subjects underwent OCT and OCTA imaging using SS-OCTA after pupil dilatation by a trained single operator. The device was PLEX Elite 9000 (Carl Zeiss Meditec Inc., Dublin, California, USA). Zeiss PLEX Elite 9000 used a 1050 nm wavelength, with scanning speed of 100,000 A-scans/second, and image process was obtained through the OCT-microangiography complex algorithm (OMAG). The acquisition protocol performed included the following scans

- OCTA map covering 6x6 mm optic disc
- OCTA map covering the center 3x3 mm macular area
- A high-definition horizontal 16 mm line scan included the fovea and ONH

All OCTA image were automatic segmentations and manual corrections were applied.

### **3.5.2 Data analytical process**

#### **3.5.2.1 Radial peripapillary capillaries vessel density**

An OCTA maps covering 6x6 mm disc area was used for quantitative analysis of RPCs microvasculature. Peripapillary evaluation was performed at the level of RPCs. Quantitative analysis of RPCs plexus was vessel density using Vessel analysis plugin version 1.1 in ImageJ software, version 1.52a (<http://imagej.nih.gov/ij/>; provided in the public domain by National Institutes of Health, Bethesda, MD, USA). For RPCs evaluation all images were automatic default threshold available in the ImageJ software to neutralize noise of the background. The image was then

converted into a binarized black and white image. The binarized image was used to create a skeletonized image. In skeletonized image all vessels even large vessels or tiny vessels were turned into only one pixel wide. The skeletonized image was examined using vessel analysis plugin for evaluated vascular density (see [Figure 1](#)). To evaluate the RPCs vessel density, we divided RPCs in to 6 quadrants; superotemporal, superonasal, nasal, inferonasal, inferotemporal and temporal quadrants (see [Figure 2](#)).

### **3.5.2.2 Foveal Avascular Zone**

An OCTA maps covering 3x3 mm macular area was used to evaluated the FAZ on both SCP and DCP. The FAZ was manually outline in SCP and DCP, the SCP slab was segmented between internal limiting membrane (ILM) and inner plexiform layer (IPL), while DCP slab extended from the IPL to the retinal pigment epithelium (RPE) (see [Figure 3](#))

### **3.5.2.3 Foveal macular thickness**

A linear 16 mm high-definition B-scan centered on the fovea were evaluated foveal macular thickness by measuring the distance between the ILM and the inner boundary of retinal pigment epithelium (RPE) (see [Figure 4](#)).

### **3.5.2.4 Vitreous degeneration and Posterior vitreous detachment**

In this study, the SS-OCT imaging were used to evaluate PVD. The HD spotlight 1 protocol was used to evaluated the vitreous, consisting of 1024 A-scans per B-scan, covering a horizontal 16 mm wide section centered on the fovea and optic disc. Visualization of the vitreous was enhanced by changing the image contrast and exposure ([Figure 5](#)). The scans were repeated 100 times to create an OCT image.

The stage of PVD was classified based on the classification system described by Itakura et al.(4) (Figure 6) :stage 0 – no PVD; stage 1 – parafoveal PVD; stage 2 – perifoveal PVD; stage 3a – vitreofoveal separation with persistent attachment to the optic disc and intact posterior precortical vitreous pocket; stage 3b – vitreofoveal separation with disrupted posterior wall of posterior precortical vitreous pocket; and stage 4 – complete PVD.

The grading of vitreous degeneration was classified based on the classification system described by Schaal et al.(5). Briefly, Grade 0 – relatively homogeneous vitreous reflectivity pattern surrounding the bursa premacularis, with or without a more central, separate lacunar space; grade 1 – vitreoschisis in the form of peripheral empty cleavage plan characterized by speckled hyperreflectivity along its borders without connection to the bursa premacularis; grade 2 – connection of the shallow empty planes with the bursa premacularis; and grade 3 – bursa premacularis and more central lacunae spaces have merged to form a larger posterior vitreous space. (see Figure 7)

### 3.6 Data analysis and statistics

Baseline characteristics of subjects were analyzed using descriptive statistics. Categorical variables were presented in number of subjects and percentage, whereas continuous variables were summarized in mean  $\pm$  standard deviation (SD) or median and range as appropriated.

Vascular density of each area, FAZ and foveal macular thickness (FMT) were summarized in mean  $\pm$  standard deviation (SD) and 95% confidence interval (CI) according to eye side and age group. Comparing between right and left eye was done using paired t-test.

Factors associated with FAZ in SCP, FAZ in DCP and FMT were explored using univariate mixed-effect linear regression model. Multivariate analysis adjusted for age and gender were performed.

Comparison of grading of vitreous degeneration and stage of posterior vitreous detachment between male and female in each age group were done using fisher's exact test.

P-value less than 0.05 was consider statistically significant. All analysis was performed by Stata software version 15.1 (Stata Corp, College Station, Texas, USA)

### **3.7 Ethical considerations**

This study conducted according to the principles of the Helsinki Declaration and in accordance with the Medical Research Involving Human Subjects Act. The study protocol was approved by Institutional Review Boards of Chulalongkorn University before it was conducted. Three fundamental ethical principles from Belmont report which including respect for persons and confidentially, beneficence and non-maleficence, and justice was applied in this study.

#### **3.7.1 Respect for person**

All eligible participants were informed by principle investigator in details about the study objectives and procedure, benefits, and risk of the study as in the participant's information sheets. Eligible participants could ask any unclear information related to the study during the information giving process and had time about 15 to 30 minutes to make the decision by themselves. If they agreed to participate in the study, they had to sign informed consent and had the right to withdraw from the study at any time.

### **3.7.2 Confidentiality**

The participants' information were protected by using the study ID to identify the individuals instead of name and hospital number. All confidential data (i.e., hospital number, date of birth, name and surname) and contact information (i.e., address, telephone number, e-mail) were kept in individual participant's log sheet with link coded which only the principle investigator who have password can access to this data. The paper documents were kept securely in the locked filing cabinet and electronic database was restricted access with a password protected computer. The data in the case record forms will be kept for 5 years and then will be destroyed by shredding at the end of the research project. All study data can be accessed by only the principle investigator and the database manager. Participants will not be identified in any reports/publications resulting from this research.

### **3.7.3 Beneficence/Non-maleficence**

This study was conducted to find the normative data of RPCs density in healthy adult eyes, so the participants didn't get the benefit from this study directly. However, result of this study can be further applied as reference for early diagnosis for optic nerve head diseases and/or retinal diseases in future.

The possible risks of harm in this study was physical discomfort mydriatic agent (i.e., temporary blur vision, eye sensitive to light, eye redness) and from the Swept-source light. (i.e., temporary blur vision) However, physical discomfort is occurred for a few minutes to a few hours after the procedure.

### **3.7.4 Justice**

All participant would undergo complete ocular examination (i.e., anterior segment examination, intraocular pressure measurement, fundus examination) and the

participants will know the normal and abnormal conditions of their eyes. Furthermore, they received the compensation of 300 Thai Baht for losing of time and transporting cost.

### **3.8 Risk and investigation responsibility**

Risk to participants was low due to all investigation, including fundus photography, optical coherence tomography angiography was used in common practice nowadays.



## CHAPTER IV

### RESULTS

The main objective of this study was to evaluate the optic nerve head microvasculature in healthy adult eyes. The secondary objectives were to evaluate macular microvascular measurement, FMT, vitreous degeneration and PVD classification in healthy adult eyes using SS-OCTA. All subjects in this study were healthy volunteers from King Chulalongkorn Memorial Hospital. Altogether, 224 eyes from 112 healthy subjects were included in this study. The demographic data of all subjects were shown in [Table 1](#). The mean age of the participants was  $48.9 \pm 15.6$  years. BCVA of all subjects were greater than 20/70 by standard EDTRS chart. Only 7 subjects were current smoking and 15% were alcohol drinking.

#### 4.1 Radial Peripapillary Capillaries vascular density

The values of radial peripapillary capillaries vascular density in 6 quadrants (Superonasal, Superotemporal, Temporal, Inferotemporal, Inferonasal and nasal quadrant) were shown in [Table 2](#). RPCs vessel density was the most crowded at inferotemporal quadrant in all age groups with mean $\pm$ SD vessel density of  $17.99 \pm 2.00$  (95% CI 17.62, 18.37) and  $17.53 \pm 2.01$  (95% CI 17.16, 17.99) for right eyes and left eyes, respectively. The lightest quadrant was nasal quadrant, mean $\pm$ SD of RPCs vessel density was  $14.20 \pm 1.82$  (95% CI 13.86, 14.54) and  $14.34 \pm 1.84$  (95% CI 13.99, 14.68) for right and left eyes, respectively. The significant differences of mean RPCs vessel density between right and left eye were seen in these two areas with p-value of 0.037 and 0.041, respectively, but there were no statistically differences of RPCs



vessel density between both eyes in superonasal, superotemporal, inferonasal and nasal quadrant. (see [Table 2](#) and [figure 8](#))

[Table 3](#) showed the mean $\pm$ SD of RPCs vessel density according to the different age groups. For participants in younger age group, defined as 20 to 40 years of age, mean RPCs vessel density at superonasal, superotemporal, temporal, inferotemporal, inferonasal, and nasal quadrant for right eye were 15.12 $\pm$ 1.39, 16.84 $\pm$ 1.85, 17.49 $\pm$ 1.65, 18.04 $\pm$ 2.13, 15.32 $\pm$ 1.78, and 14.25 $\pm$ 1.79, respectively, and 15.13 $\pm$ 1.64, 16.83 $\pm$ 2.45, 17.55 $\pm$ 2.06, 17.36 $\pm$ 2.64, 15.34 $\pm$ 1.49, and 14.88 $\pm$ 1.51 for left eye, respectively. For participants in middle age group, defined as 41 to 60 years of age, mean RPCs vessel density at superonasal, superotemporal, temporal, inferotemporal, inferonasal, and nasal quadrant for right eye were 15.10 $\pm$ 1.56, 17.23 $\pm$ 2.18, 17.27 $\pm$ 1.90, 17.87 $\pm$ 2.35, 15.35 $\pm$ 1.70, and 14.44 $\pm$ 1.69, respectively, and 14.84 $\pm$ 1.54, 17.05 $\pm$ 2.18, 17.72 $\pm$ 1.94, 17.69 $\pm$ 2.17, 15.22 $\pm$ 1.71, and 14.29 $\pm$ 2.00 for left eye, respectively. For participants in older age group, defined as 61 years of age and older, mean RPCs vessel density at superonasal, superotemporal, temporal, inferotemporal, inferonasal, and nasal quadrant for right eye were 14.50 $\pm$ 2.12, 16.85 $\pm$ 2.00, 16.55 $\pm$ 2.32, 18.07 $\pm$ 1.24, 14.49 $\pm$ 1.83, and 13.89 $\pm$ 1.97, respectively, and 14.56 $\pm$ 1.78, 17.13 $\pm$ 1.90, 17.16 $\pm$ 1.78, 17.16 $\pm$ 1.74, 14.68 $\pm$ 2.13, and 13.81 $\pm$ 1.87 for left eye, respectively.

#### **4.2 Foveal Avascular Zone (FAZ) and Foveal Macular Thickness (FMT)**

The mean  $\pm$  SD of SCP- FAZ were 0.31  $\pm$ 0.1 mm<sup>2</sup> (95% CI of 0.29, 0.33) and 0.30  $\pm$  0.1 mm<sup>2</sup> (95% CI of 0.29, 0.32) from right eyes and left eyes, respectively.

Mean  $\pm$  SD of FAZ in DCP were 0.56  $\pm$ 0.22 mm<sup>2</sup> (95% CI of 0.52, 0.60) and 0.56  $\pm$

0.21 mm<sup>2</sup> (95% CI of 0.52, 0.60) from right eyes and left eyes, respectively. Thickness of FMT were 379.48 ± 37.66 μm (95% CI of 372.43,386.53) and 382.04 ± 36.61 μm (95% CI of 375.19, 388.90) from right eyes and left eyes, respectively (Table 4). There was no statistically significant different of SCP-FAZ, DCP-FAZ and foveal macular thickness between both eyes. Table 5 showed the foveal microvascular measurement according to the different age groups. For participants in young age group, SCP-FAZ, DCP-FAZ, and FMT of right eye were 0.26 ± 0.10 mm<sup>2</sup>, 0.43 ± 0.16 mm<sup>2</sup>, and 385.58 ± 31.28 μm, respectively, and 0.26 ± 0.09 mm<sup>2</sup>, 0.43 ± 0.15 mm<sup>2</sup>, and 380.89 ± 31.44 μm for left eye, respectively. For participants in middle age group, SCP-FAZ, DCP-FAZ, and FMT of right eye were 0.31 ± 0.10 mm<sup>2</sup>, 0.55 ± 0.22 mm<sup>2</sup>, and 382.45 ± 40.99 μm, respectively, and 0.31 ± 0.10 mm<sup>2</sup>, 0.55 ± 0.19 mm<sup>2</sup>, and 390.63 ± 39.43 μm for left eye respectively. For participants in older age group, SCP-FAZ, DCP-FAZ, and FMT of right eye were 0.35 ± 0.10 mm<sup>2</sup>, 0.71 ± 0.17 mm<sup>2</sup>, and 369.92 ± 39.27 μm, respectively, and 0.34 ± 0.11 mm<sup>2</sup>, 0.71 ± 0.17 mm<sup>2</sup>, and 374.19 ± 37.63 μm for left eye respectively.

The data showed that FAZ at superficial and deep capillary plexus were greater in elderly age group. On the other hand, the thickness of FMT was decrease in elderly age group.

From univariate analysis, age was significant predictive factor of SCP-FAZ with beta coefficient of 0.002 (95% CI of 0.001, 0.004), p<0.001. After adjusted with age, sex, FMT, and smoking status in multivariate mixed-linear regression analysis, only age and sex were significant predictive factors associated with SCP-FAZ. The result showed that age had positively correlation with the area of SCP-FAZ (beta coefficient 0.002 (95% CI of 0.001, 0.003), p<0.001). Female had higher SCP-FAZ

area compared to male with beta coefficient (95% CI) of 0.035 (0.003, 0.070),  $p = 0.047$ . (see [Table 6](#))

In univariate analysis, age, sex and refractive error were significant predictive factor of DCP-FAZ with beta coefficient (95% CI) of 0.007 (0.005, 0.009),  $p < 0.001$ , -0.081 (-0.157, -0.005),  $p = 0.037$  and 0.167 (0.085, 0.248),  $p < 0.001$ , respectively. After adjusted with age, sex, FMT, refractive error and smoking status in multivariate mixed-linear regression analysis, only age and sex were significant predictive factors associated with DCP-FAZ. The result showed that age had positively correlation with the area of DCP-FAZ with beta coefficient (95% CI) of 0.005 (0.002, 0.008),  $p < 0.001$ . Female had lower DCP-FAZ area compare to male with beta coefficient (95% CI) of -0.071(-0.136, -0.007),  $p = 0.029$ ). (see [Table 7](#))

For FMT, in univariate analysis, age was significant predictive factor of the thickness of FMT with beta coefficient (95% CI) of -0.410 (-0.801, -0.018),  $p < 0.004$ . After adjusted with age and sex in multivariate mixed-linear regression analysis. Age was significant predictive factors associated with FMT. The result showed that age had inverse correlation with the thickness of FMT with beta coefficient (95% CI) of -0.424 (-0.813, -0.034),  $p = 0.033$ ). (see [Table 8](#))

### **4.3 Posterior Vitreous Detachment (PVD)**

The vitreous degeneration was graded according to the criteria proposed by Schaal.(5) Using SS-OCT, there were 43 eyes that non-gradable, who had low scan quality or previous posterior vitreous detachment. At 20 to 40 years of age, most of eyes had relatively homogeneous vitreous and the percentage of eye with homogeneous vitreous was 71%. At 41 to 61 year of age, most of eyes had vitreoschisis in the form of peripheral empty cleavage plan (48%). At 61 year of age

and older, the premacular bursa had connected/merged to form a larger posterior vitreous space, the percentage of grade 3 was 17%. There was statistically significant correlation between age and grading of vitreous degeneration ( $P < 0.001$ ). (See [Table 9](#) and [Figure 9](#))

In Our study, we classified PVD into 5 groups according to the biomicroscopic finding as describe as above. Using SS-OCT, posterior precortical vitreous pocket (PPVP) were seen in all 175 eyes without complete PVD. Our study found that stage of posterior hyaloid status was associated with age. There was more advanced stage in participant in older age group. Thirty-four subjects (89%) in younger age group were stage 0, whereas 32 (47%) of subjects in middle age group were stage 1, and 40 (57%) of participants in older age group were stage 4 complete PVD. (See detail in [Table 9](#) and [Figure 10](#))

The staging of PVD was significantly associated with the age group ( $P < 0.001$ ). At 20 to 40 years of age, the percentage of eyes with no PVD and paramacular PVD was 86% and 10%, respectively, in female and 94% and 6%, respectively, in the male. At 41 to 60 year of age, the percentage of eyes with no PVD and paramacular PVD was 27% and 43%, respectively, in female and 47% and 41%, respectively, in the male. At 61 year of age and older, the percentage of eyes with complete PVD was 50% in female and 61% in the male. The staging of PVD did not significantly different between the female and male in all age groups. (see [Figure 11](#))

## CHAPTER V

### DISCUSSION, CONCLUSION AND SUGGESTIONS

#### 5.1 Discussion

##### 5.1.1 Radial Peripapillary Capillaries vascular density

The objective of this study was to define clinical normative data of RPCs density using PLEX Elite 9000 SS-OCTA. By the advancement of SS-OCTA technology, the RPCs can be clearly visualized. The normative data was necessary for the use of SS-OCTA in clinical practice. Normative RPCs density data was needed to use as reference data and use to compare between healthy individuals to patients who had pathology of optic nerve or retina abnormalities.

In this study, we used the SS-OCTA device to obtain image and using ImageJ software to quantify RPCs density data. We found that inferotemporal quadrant was the most crowded quadrant of RPCs vessel density whereas nasal quadrant was the lightest quadrant of RPCs vessel density.

Our study showed that the RPCs density was crowded in the arcuate regions (superotemporal and inferotemporal quadrant) than in other areas which similar to study reported by Rao et al., higher density of RPCs was seen in inferotemporal and superotemporal quadrant(32). In study of Bazvand et al. showed that the highest RPCs density was recorded in the inferotemporal quadrant(33). Fernandez-vigo et al. analysed RPCs in 4 quadrants (i.e., superior, inferior, temporal and nasal quadrant) and found that the highest RPCs was recorded in the inferior quadrant(34).

Mase et al. reported that the RPCs density gradually decreased from the peripapillary area to the peripheral area(35). Yu et al. reported that RPCs volume generally positively correlated with the RNFL thickness in healthy eyes(36). With the current reports, the thicker RNFL has a denser RPCs, suggesting that the RPCs may be a primarily responsible for RNFL nourishment.

In this study, we found significant difference in RPCs density between both eyes in temporal and inferotemporal quadrant. ( $p=0.037$  and  $0.041$ , respectively). Hou et al. conducted study in healthy eyes, glaucoma suspected patients, and patients with bilateral glaucoma. Asymmetry of RPCs density between both eyes was seen in 1.7% of healthy individuals and 2.2% of glaucomatous patients. But no significant different in asymmetry of RNFL thickness were found in healthy eyes(37).

However, the result of RPCs density from different OCTA algorithms cannot be compared or interchangeable use to follow-up patients because of the difference dimensions and the depth of the area of interest which was assessed(38). Thus, to compare the results across OCTA devices and techniques should be considered with caution.

### **5.1.2 Foveal Avascular Zone (FAZ) and Foveal Macular Thickness (FMT)**

FAZ is a small capillary-free area with contained of high density of photoreceptor. Many of studies found that the size of FAZ did not seem to affect visual function in healthy eyes(39-41). Some of them believes that alteration of FAZ could be potential markers of foveal function.

Our study found that age and sex were significant predictive factors associated with the area of FAZ. Age had positively correlation with the area of SCP-FAZ and

DCP-FAZ. There was different correlation of the area of FAZ between male and female. Female had higher SCP-FAZ area compared to male, while, male had higher DCP-FAZ area compared to female. For FMT, the study showed that age had negatively correlation with the thickness of FMT.

In this study, the mean  $\pm$  SD of SCP-FAZ were  $0.31 \pm 0.1 \text{ mm}^2$  and DCP-FAZ were  $0.56 \pm 0.22 \text{ mm}^2$ . From previous study, the values of SCP-FAZ in healthy eyes by using OCTA ranging from  $0.251 \pm 0.096 \text{ mm}^2$  to  $0.474 \pm 0.172 \text{ mm}^2$  and DCP-FAZ ranging from  $0.298 \pm 0.108 \text{ mm}^2$  to  $0.614 \pm 0.2 \text{ mm}^2$  (9, 26, 27, 39, 42-56). (See detail in [Table 10](#)) Falavarjani and colleagues reported mean SCP-FAZ and DCP-FAZ to be  $0.32 \text{ mm}^2$  and  $0.50 \text{ mm}^2$ , respectively, which is similar to our findings.(56) The variability of FAZ area may be explained by difference in the study population, study devices, and software or methods of measurements. All previous studies found that DCP-FAZ was larger than SCP-FAZ. A consistent finding data from previous studies was a larger DCP-FAZ than SCP-FAZ. The larger size of DCP-FAZ will be explained by the unique relationship of capillary plexus at fovea (i.e. the capillary plexuses intersect at the fovea). At deep capillary plexus layers, the vessels are moving into the inner plexiform layers (IPL)/ganglion cell layers which is anatomic layers narrow at the fovea. The segmentation may break down at the foveal because of the capillaries in DCP layers were laminar and intersect only with vertical connecting vessels(44).

FAZ may influence by sex. This study found that female had higher SCP-FAZ area compared to male, on the other hand, male had higher DCP-FAZ area compared to female. Samara et al., Coscas et al. and Alnawaiseh et al. found no significant differences in macular microvasculature (including flow density and FAZ area) in

both sexes(39, 44, 57). On the contrary, Tan et al. and Yu et al. reported a larger FAZ area in female than in male(26, 53). Yu et al., conducted study in Chinese population, reported that the capillary free zone area is significant larger in females than in male (0.52 mm<sup>2</sup> versus 0.42 mm<sup>2</sup>, p = 0.012). (53) Gomez-Ulla and colleagues found that the FAZ area in female is significant larger (mean 0.297 mm<sup>2</sup>) than in male (mean 0.254 mm<sup>2</sup>)(55). As we know that the estrogen, androgen and progesterone receptors are present in the eyes and these steroid hormones are produced in ocular tissues. Sex hormones may play a role on the retina and ocular blood flow. In agreement with previous studies, our results also show that FAZ areas influenced by sex. Our studies found that female had larger SCP-FAZ area than male. While female had lower DCP-FAZ compare to male. Different OCT-A devices and measurement method may be the cause of these discrepancies.

Age was a crucial factor that effect in anatomical changes in the macular region. Our study shown that age was significant predictive factors associated with SCP-FAZ, DCP-FAZ, and FMT. For SCP-FAZ and DCP-FAZ, age had positively correlation, while negatively correlation with the thickness of FMT. Nowadays, the influence of age on FAZ area are unclear. Samara et al. and Wang at al. found no relationship between age and FAZ area with similar to the reported from Tan et al. and Linderman et al.(26, 39, 49, 58). Whereas some of studies found relationship between age and FAZ. Wu et al. using FA to study FAZ in normal eyes, found a positive correlation between FAZ and age.(59) Study in Chinese population by Yu et al. showed that FAZ area increased by average 1.48% per year accompanied by decrease in vascular density by 0.4% per year(53). Coscas and colleague conducted study in 135 eyes in three age groups, 20-39 years, 40-59 years, and 60 years or older.



They found that the SCP-FAZ area was significantly smaller in older subjects.(44) Song et al. analysed images from OCT and reported that retinal thickness declines with age(60). However, Adhi et al. and Sull et al. reported that no relationship between age and foveal thickness(61, 62). In this study, we found that the FMT was decrease in elderly participants. There was few studies evaluated the effect of FMT on FAZ area(39, 52). We found no significant correlation between FMT and FAZ area, both SCP-FAZ and DCP-FAZ. Ghassemi et al. reported that SCP-FAZ and DCP-FAZ had an inverse relationship with FMT after adjusting with age and gender.(63) While Samara et al. reported that FMT was inversely correlated with both SCP-FAZ and DCP-FAZ, but not correlated with age and gender.(39) Tan et al. reported that the FAZ area was affected by FMT and gender only.(26) So, the relationship between FMT and FAZ could not be concluded.

### **5.1.3 Posterior Vitreous Detachment (PVD)**

PVD is a condition of the eye that has been thought to be an liquefied fluid run through a break in the vitreous cortex into the retrohyaloid space(4). According to the advances in technology, SS-OCT offer a high-quality vitreous image that can revealed more detail in various vitreous spaces (premacular bursa, Cloquet's canal, and prevascular fissures and cisterns).

This study used the SS-OCT and found that higher PVD stage was significant associated with increasing age. Our study found that subjects in younger age group (20-40 years) had lower stage of PVD, 97% had no PVD and paramacular PVD. While 19% of subjects in older age group ( $\geq 61$  years) had no PVD and paramacular PVD. The frequency of complete PVD was highest in subjects in older age group ( $\geq 61$  years), 53%, compared to none in younger age group (20-40 years). In our study,

we found that there was not significantly different of PVD stage between male and female in all age groups.

Previously studies on the vitreous studies, chuo et al. and Shen et al. studied about prevalence and risk factors of PVD using indirect retinoscopy(64, 65). The result showed that the prevalence of PVD was greater in female than in male. More recent study, Schwab et al. used SD-OCT and ultrasound B-scan to studied stage of OVD in healthy eye, reported that no significant difference in the PVD stage between male and female(66). Hayashi et al. used SS-OCT to demonstrate factors associated with the progression of PVD staging, the result showed that PVD significantly progressed with increasing age in both genders and occurred significantly faster in female than in male at 60 years of age and older.(67) Our study had similar result to Hayashi's study, we found that lower PVD stage was significantly higher in younger subjects while higher PVD stage was seen in older subjects, but there was no significant difference between male and female. To our knowledge some of retinal diseases associated with the progression of PVD, including retinal break/tear, macular holes, vitreomacular traction syndrome, rhegmatogenous retinal detachments(68-71). The incidence of macular hole occurred more frequently in women than in men(72-75). The studies from Itakura et al. and Kakehashi et al. reported that a perifoveal PVD was seen frequently in cases of idiopathic macular holes(4, 76). Our study found that the frequency of perifoveal PVD was about 3 times higher in female than male. (74% versus 26%).

Schaal et al. described the anatomical features seen with the posterior vitreous and proposed a grading of vitreous degeneration based on the premacular bursa and its relationship to various lacunae and degenerative cleavage/plans within the

vitreous(5). In our study, 23 eyes were non-degradable for vitreous degeneration grading. This study found that 71% and 0% of relative homogeneous vitreous reflectivity pattern surrounding the premacular bursa at 20 to 40 years of age and at 61 years of age and older, respectively. While vitreoschisis was found 83% and 100% at 40 to 60 years of age and at 61 year of age and older, respectively. This study revealed the progression of vitreous degeneration grading significantly with increasing age. These finding suggested that vitreous degeneration generally begin to progress at 40 year of age and gradually progress with increasing age. This result was similar to previous studies, Itakura and colleague and Hayashi et al. reported that vitreous degeneration generally begins to progress at 40 years of age(4, 67).

## **5.2 Conclusion**

### **5.2.1 Radial Peripapillary Capillaries vascular density**

SS-OCTA imaging can clearly visualized the expansion of the RPCs, which distributed to the superficial peripapillary retina. Density of the RPCs in healthy eyes from our study can be considered as a standard map of the RPCs and compare to those eyes with retina vascular disorders.

### **5.2.2 Foveal Avascular Zone (FAZ) and Foveal Macular Thickness (FMT)**

In our study, we demonstrated SCP-FAZ, DCP-FAZ, and FMT in healthy Thai population. The data shown that SCP-FAZ was larger than DCP-FAZ. Age influenced on the size of FAZ area, both SCP-FAZ and DCP-FAZ were larger in older subjects than young subjects. For FAZ, female had higher SCP-FAZ area compared to male, while, male had higher DCP-FAZ area compared to female. For

FMT, the thickness of FMT had significant inverse correlation with age. We found no significant correlation between both FAZ area and FMT.

### 5.2.3 Posterior Vitreous Detachment (PVD)

Advance OCT technology, SS-OCT imaging revealed the variable morphology of posterior vitreous structures and the progression of PVD. PVD progression was significantly with increasing age regardless of gender.

### 5.3 The strengths of this study

This study was the first study that used the Zeiss PLEX Elite 9000 SS-OCT to assess the normative data in Thai healthy eyes. The Zeiss PLEX elite 9000 provided the SS-OCT resolution and the clear image of the posterior structure of the eyes among other currently available OCTs devices.

### 5.4 The limitation of this study

This study had some limitations. First, a cross-sectional design without follow-up data limits our ability to draw conclusion about the effect of increasing age on study variables. Further follow-up of patients is necessary to assess the longitudinal changes in radial peripapillary capillaries vascular density, FAZ, FMT, and PVD stage as subjects age increase. Second, only subjects with small refractive errors (-3 to +3 diopters) were included, so the effects of high level of myopia or hyperopia on the foveal microvasculature were not evaluated. Third, axial length, foveal morphology, and foveal vascular density were not included in this study.

## 5.5 Suggestion

Our study gives the SS-OCT/OCTA normative database using the PLEX Elite 9000 device of RPCs density, FAZ area, FMT thickness and PVD staging in healthy eyes of Thai people. This baseline database of healthy eyes may used to help for detect, early diagnosis or monitor in the pathologic eyes. Further investigation in pathologic eye is needed.



Figure 1 Acquisition image

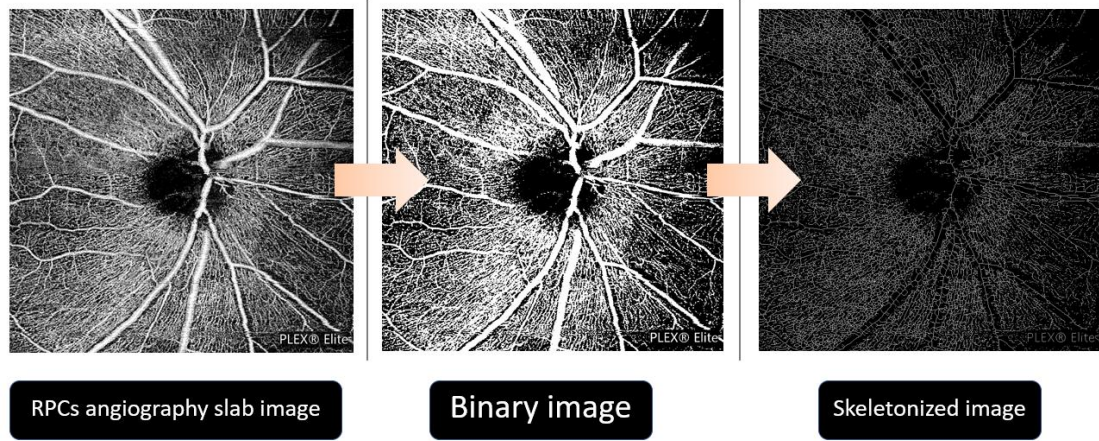
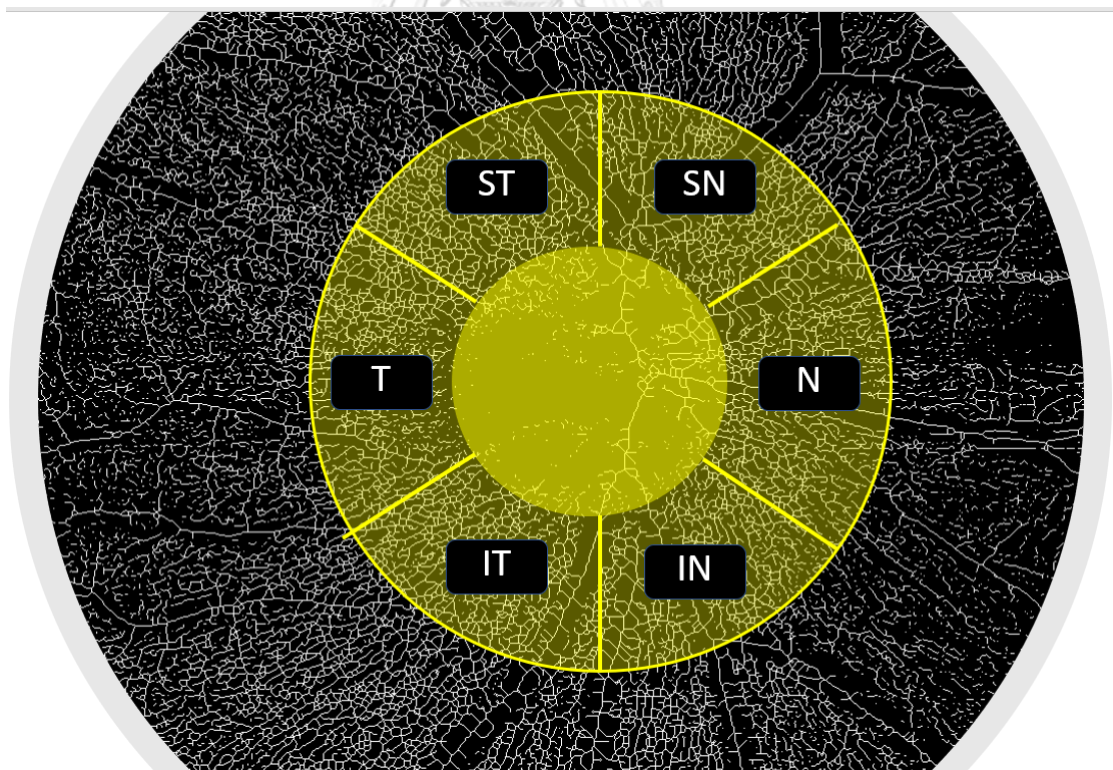
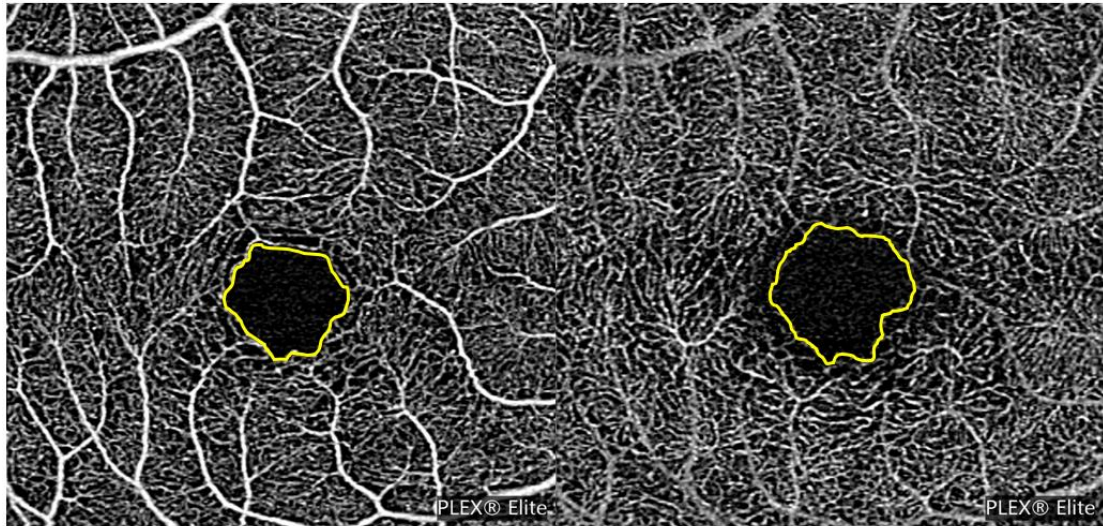


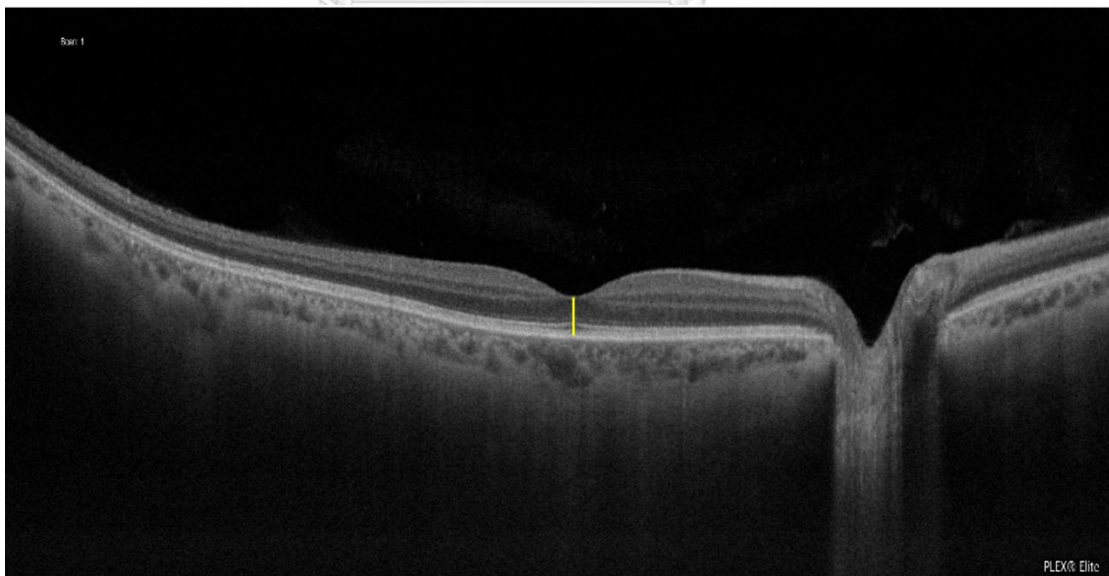
Figure 2 Quadrant of RPCs



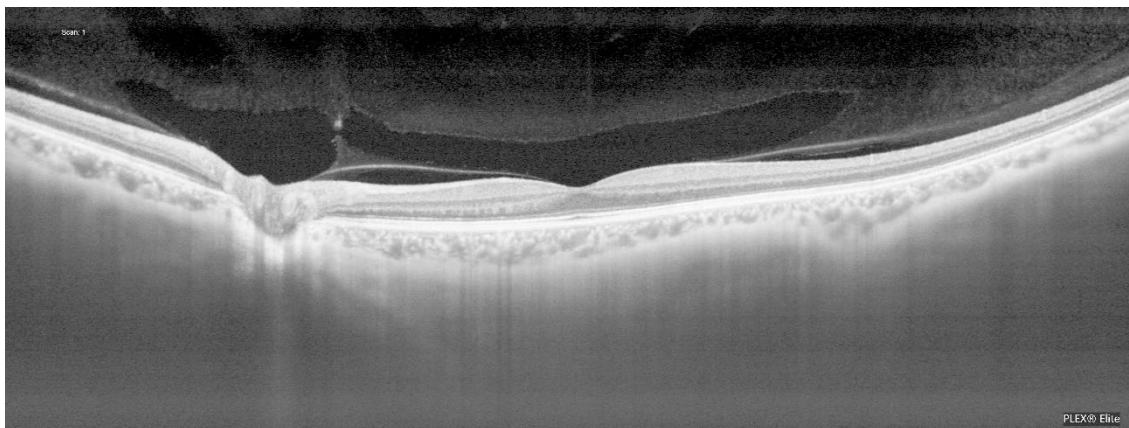
*Figure 3 An OCTA maps 3\*3 mm macular area (A-SCP, B-DCP)*



*Figure 4 A linear 16 mm high-definition B-scan centered on the fovea for foveal macular thickness evaluation*

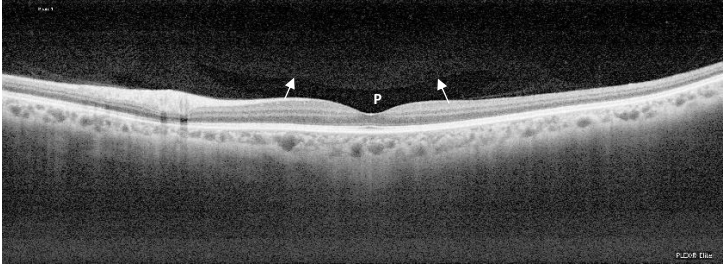

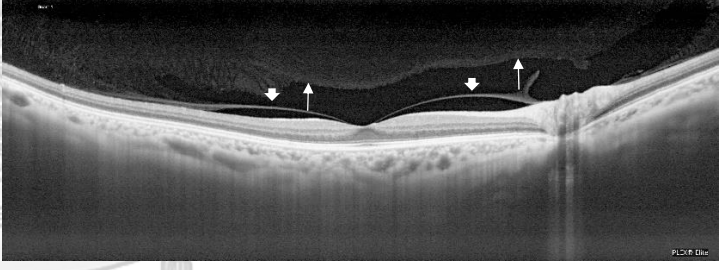
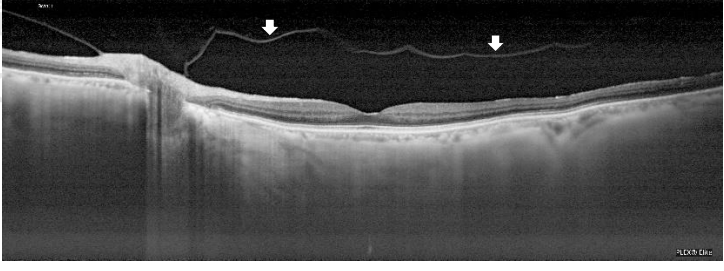
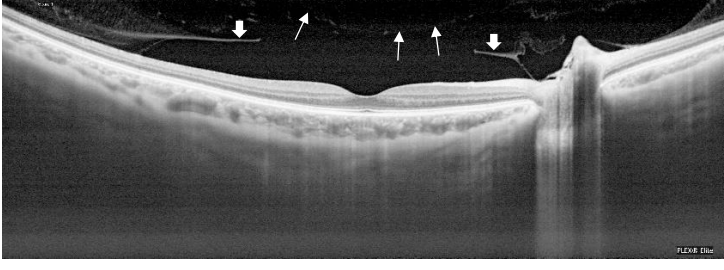


*Figure 5 The SS-OCT imaging used for PVD evaluation*

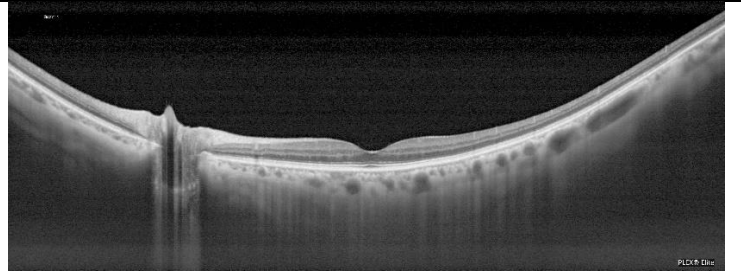




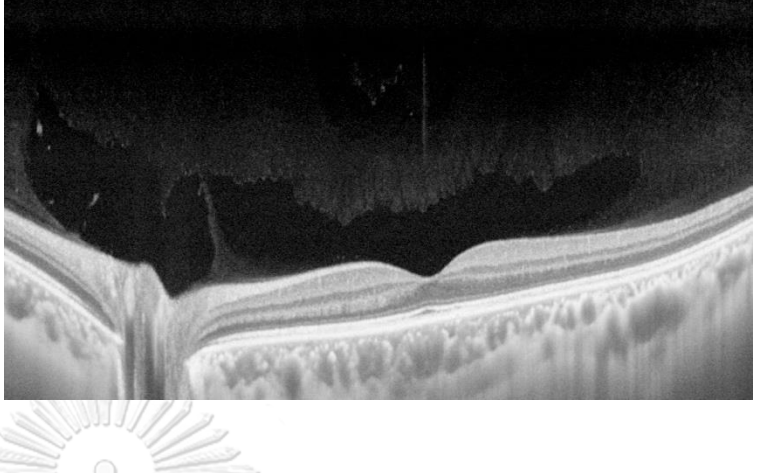
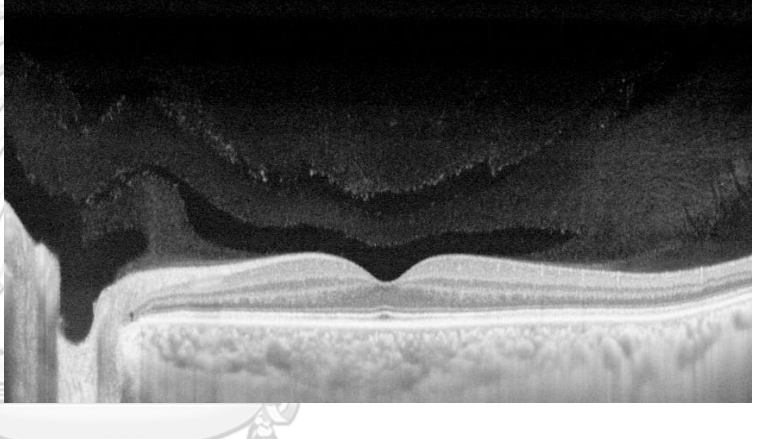
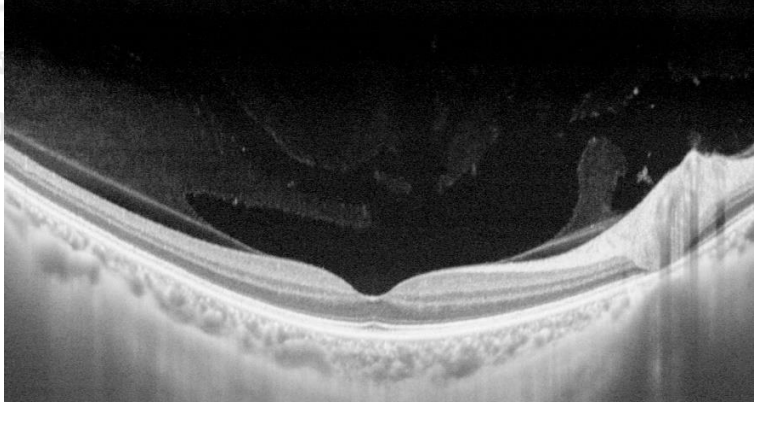
*Figure 6 Stage of PVD Development*

|   |  |
|---|--|
| <p><b>Stage 0:</b> no PVD</p>   |    |
| <p><b>Stage 1:</b> paramacular PVD</p>  |    |
| <p><b>Stage 2:</b> perifoveal PVD</p>   |  |
| <p><b>Stage 3a:</b> vitreofoveal separation with persistent attachment to the optic disc and intact posterior precortical vitreous pocket</p> |  |
| <p><b>Stage 3b:</b> vitreofoveal separation with disrupted posterior wall of posterior precortical vitreous pocket</p>                        |  |

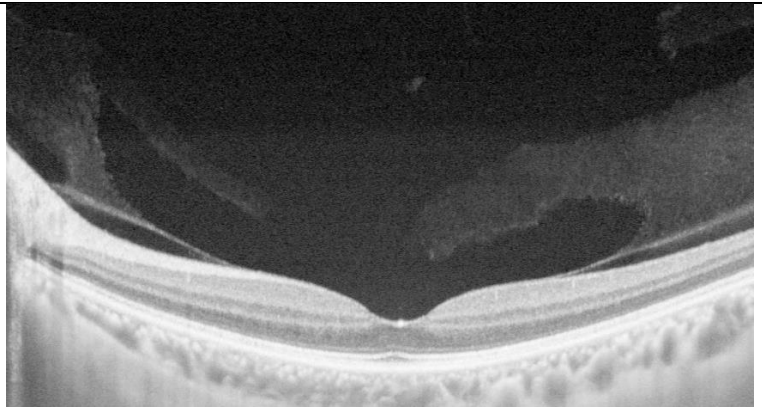
**Stage 4:** complete PVD



*Figure 7 Grading of vitreous degeneration*

|  |  |
|--|--|
| <p><b>Grade 0:</b> relative homogeneous vitreous reflectivity pattern surrounding the premacular bursa</p>   |    |
| <p><b>Grade 1:</b> vitreoschisis in the form of peripheral empty cleavage plane characterized by speckled hyperreflectivity along its borders without connection to the premacular bursa</p> |   |
| <p><b>Grade 2:</b> connection of these shallow empty planes with the premacular bursa</p>  |  |

**Grade 3:** premacular and more central lacunar spaces have emerged to form a larger posterior vitreous space



จุฬาลงกรณ์มหาวิทยาลัย  
CHULALONGKORN UNIVERSITY

*Table 1 Baseline demographic data of the 112 subjects*

| <b>Characteristics (n, %)</b>               | <b>Total (n=112)</b> |
|---|----------------------|
| <b>Sex</b>                                  |                      |
| Male  | 51 (45.5)            |
| Female                                      | 61 (54.5)            |
| <b>Age (mean <math>\pm</math> SD, yrs.)</b> | 48.9 $\pm$ 15.6      |
| <b>Age group (yrs.)</b>                     |                      |
| 20-40                                       | 38 (33.9)            |
| 40-60                                       | 38 (33.9)            |
| $\geq 61$                                   | 36 (32.2)            |
| <b>VA</b>                                   |                      |
| >20/70                                      | 112 (100.0)          |
| <b>Refractive error</b>                     |                      |
| Myopia                                      | 26 (23.2)            |
| Normal                                      | 53 (47.3)            |
| Hyperopia                                   | 3 (29.5)             |
| <b>Smoking status</b>                       |                      |
| Yes   | 7 (6.3)              |
| No  | 105 (93.7)           |
| <b>Alcohol drinking status</b>              |                      |
| Yes   | 17 (15.2)            |
| No  | 95 (84.8)            |

Table 2 Vascular density between Rt and Lt eye

| Area<br>(mean $\pm$ SD, 95% CI) | Vascular density                   |                                    | p-value |
|---------------------------------|------------------------------------|------------------------------------|---------|
|                                 | OD                                 | OS                                 |         |
| <b>Superonasal</b>              | 14.91 $\pm$ 1.72<br>(14.59, 15.24) | 14.85 $\pm$ 1.66<br>(14.54, 15.16) | 0.717   |
| <b>Superotemporal</b>           | 16.98 $\pm$ 2.01<br>(16.60, 17.35) | 17.00 $\pm$ 2.18<br>(16.59, 17.41) | 0.914   |
| <b>Temporal</b>                 | 17.11 $\pm$ 1.99<br>(16.74, 17.49) | 17.48 $\pm$ 1.93<br>(17.12, 17.84) | 0.037   |
| <b>Inferotemporal</b>           | 17.99 $\pm$ 2.00<br>(17.62, 18.37) | 17.53 $\pm$ 2.01<br>(17.16, 17.99) | 0.041   |
| <b>Inferonasal</b>              | 15.21 $\pm$ 1.76<br>(14.88, 15.54) | 15.15 $\pm$ 1.81<br>(14.81, 15.49) | 0.753   |
| <b>Nasal</b>                    | 14.20 $\pm$ 1.82<br>(13.86, 14.54) | 14.34 $\pm$ 1.84<br>(13.99, 14.68) | 0.444   |

\*Paired t-test

Table 3 Normative data of vascular density

| Area<br>(mean $\pm$ SD) |    | Age group (yrs.) |                  |                   |
|-------------------------|----|------------------|------------------|-------------------|
|                         |    | 20-40            | 41-60            | $\geq 61$         |
| <b>Superonasal</b>      | OD | 15.12 $\pm$ 1.39 | 15.10 $\pm$ 1.56 | 14.50 $\pm$ 2.12  |
|                         | OS | 15.13 $\pm$ 1.64 | 14.84 $\pm$ 1.54 | 14.56 $\pm$ 1.78  |
| <b>Superotemporal</b>   | OD | 16.84 $\pm$ 1.85 | 17.23 $\pm$ 2.18 | 16.85 $\pm$ 2.00  |
|                         | OS | 16.83 $\pm$ 2.45 | 17.05 $\pm$ 2.18 | 17.13 $\pm$ 1.90  |
| <b>Temporal</b>         | OD | 17.49 $\pm$ 1.65 | 17.27 $\pm$ 1.90 | 16.55 $\pm$ 2.32  |
|                         | OS | 17.55 $\pm$ 2.06 | 17.72 $\pm$ 1.94 | 17.16 $\pm$ 1.78  |
| <b>Inferotemporal</b>   | OD | 18.04 $\pm$ 2.13 | 17.87 $\pm$ 2.35 | 18.07 $\pm$ 1.42  |
|                         | OS | 17.36 $\pm$ 2.64 | 17.69 $\pm$ 2.17 | 17.16 $\pm$ 1.74  |
| <b>Inferonasal</b>      | OD | 15.32 $\pm$ 1.78 | 15.35 $\pm$ 1.70 | 14.49 $\pm$ 11.83 |
|                         | OS | 15.34 $\pm$ 1.49 | 15.22 $\pm$ 1.71 | 14.68 $\pm$ 2.13  |
| <b>Nasal</b>            | OD | 14.25 $\pm$ 1.79 | 14.44 $\pm$ 1.69 | 13.89 $\pm$ 1.97  |
|                         | OS | 14.88 $\pm$ 1.51 | 14.29 $\pm$ 2.00 | 13.81 $\pm$ 1.87  |

Figure 8 Box plot of vascular density between Rt and Lt eye

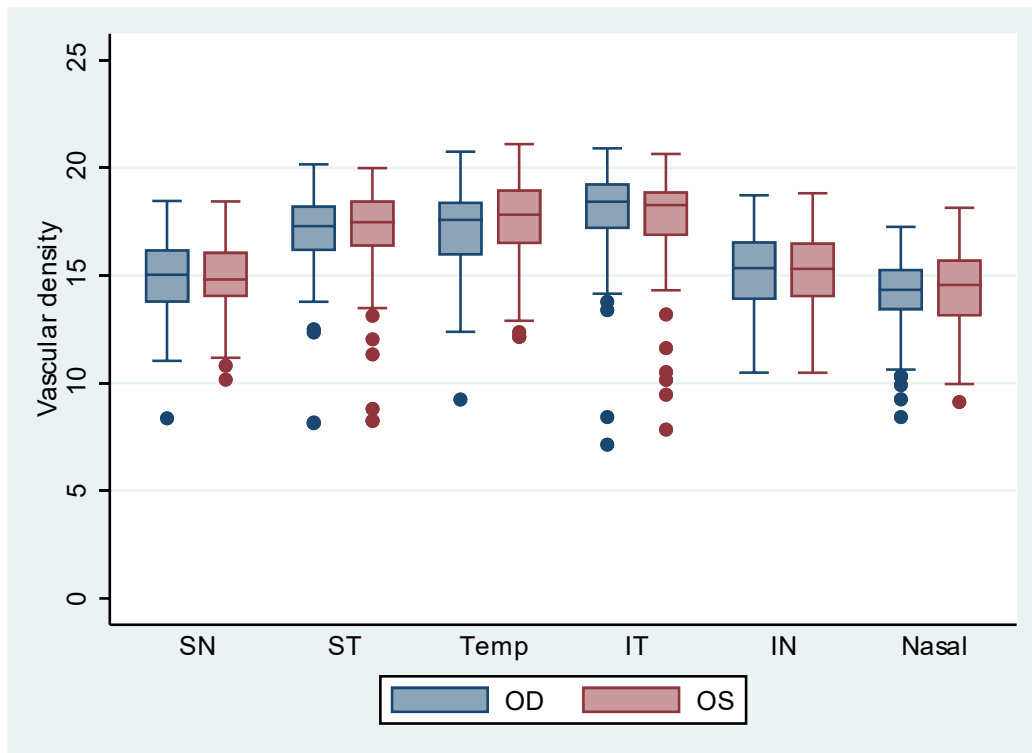


Table 4 Mean foveal avascular zone and foveal macular thickness according to eye side

| (mean $\pm$ SD, 95% CI)         | Side                                   |  | p-value |
|---------------------------------|--|--|---------|
|                                 | OD                                     | OS                                     |         |
| <b>SCP-FAZ (mm<sup>2</sup>)</b> | 0.31 $\pm$ 0.10<br>(0.29, 0.33)        | 0.30 $\pm$ 0.10<br>(0.29, 0.32)        | 0.698   |
| <b>DCP-FAZ (mm<sup>2</sup>)</b> | 0.56 $\pm$ 0.22<br>(0.52, 0.60)        | 0.56 $\pm$ 0.21<br>(0.52, 0.60)        | 0.936   |
| <b>FMT (<math>\mu</math>m)</b>  | 379.48 $\pm$ 37.66<br>(372.43, 386.53) | 382.04 $\pm$ 36.61<br>(375.19, 388.90) | 0.389   |



*Table 5 FAZ and FMT in different age groups*

| (mean ± SD)                     |    | Age group (yrs.) |                |                |
|---------------------------------|----|------------------|----------------|----------------|
|                                 |    | 20-40            | 41-60          | ≥ 61           |
| <b>SCP-FAZ (mm<sup>2</sup>)</b> | OD | 0.26 ± 0.10      | 0.31 ± 0.10    | 0.35 ± 0.10    |
|                                 | OS | 0.26 ± 0.09      | 0.31 ± 0.10    | 0.34 ± 0.11    |
| <b>DCP-FAZ (mm<sup>2</sup>)</b> | OD | 0.43 ± 0.16      | 0.55 ± 0.22    | 0.71 ± 0.17    |
|                                 | OS | 0.43 ± 0.15      | 0.55 ± 0.19    | 0.71 ± 0.17    |
| <b>FMT (μm)</b>                 | OD | 385.58 ± 31.28   | 382.45 ± 40.99 | 369.92 ± 39.27 |
|                                 | OS | 380.89 ± 31.44   | 390.63 ± 39.43 | 374.19 ± 37.63 |

Table 6 Univariate and Multivariate analysis of SCP-FAZ

| Predictive factors      | Univariate analysis |                    |         | Multivariate analysis |                  |         |
|-------------------------|---------------------|--------------------|---------|-----------------------|------------------|---------|
|                         | Beta Coefficient    | 95% CI             | p-value | Beta Coefficient      | 95% CI           | p-value |
| Age                     | 0.002               | 0.001, 0.004       | <0.001  | 0.002                 | 0.001, 0.003     | <0.001  |
| Sex                     |                     |                    |         |                       |                  |         |
| Male                    | Ref                 |                    |         | Ref                   |                  |         |
| Female                  | 0.033               | -0.004, 0.071      | 0.084   | 0.035                 | 0.003, 0.070     | 0.047   |
| FMT                     | -0.0001             | -0.00029, 0.000045 | 0.154   | -0.001                | -0.0002, 0.00004 | 0.157   |
| <b>Refractive error</b> |                     |                    |         |                       |                  |         |
| Myopia                  | -0.019              | -0.065, 0.028      | 0.436   |                       |                  |         |
| Normal                  | Ref                 |                    |         |                       |                  |         |
| Hyperopia               | 0.042               | -0.001, 0.085      | 0.057   |                       |                  |         |
| <b>Smoking</b>          |                     |                    |         |                       |                  |         |
| No                      | Ref                 |                    |         | Ref                   |                  |         |
| Yes                     | -0.065              | -0.143, 0.012      | 0.099   | -0.129                | -0.086, 0.060    | 0.73    |
| <b>Alcohol</b>          |                     |                    |         |                       |                  |         |
| No                      | Ref                 |                    |         |                       |                  |         |
| Yes                     | -0.046              | -0.098, 0.006      | 0.085   |                       |                  |         |

Table 7 Univariate and Multivariate analysis of DCP-FAZ

| Predictive factors      | Univariate analysis |                   |         | Multivariate analysis |                  |         |
|-------------------------|---------------------|-------------------|---------|-----------------------|------------------|---------|
|                         | Beta Coefficient    | 95% CI            | p-value | Beta Coefficient      | 95% CI           | p-value |
| Age                     | 0.007               | 0.005, 0.009      | <0.001  | 0.005                 | 0.002, 0.008     | <0.001  |
| Sex                     |                     |                   |         |                       |                  |         |
| Male                    | Ref                 |                   |         | Ref                   |                  |         |
| Female                  | -0.081              | -0.157, -0.005    | 0.037   | -0.071                | -0.136, -0.007   | 0.029   |
| FMT                     | -0.0002             | -0.0005, 0.000067 | 0.133   | -0.0002               | -0.0005, 0.00006 | 0.127   |
| <b>Refractive error</b> |                     |                   |         |                       |                  |         |
| Myopia                  | -0.068              | -0.156, 0.021     | 0.134   | -0.344                | -0.115, 0.046    | 0.403   |
| Normal                  | Ref                 |                   |         | Ref                   |                  |         |
| Hyperopia               | 0.167               | 0.085, 0.248      | <0.001  | 0.061                 | -0.025, 0.147    | 0.167   |
| <b>Smoking</b>          |                     |                   |         |                       |                  |         |
| No                      | Ref                 |                   |         | Ref                   |                  |         |
| Yes                     | -0.089              | -0.247, 0.070     | 0.273   | -0.100                | -0.146, 0.126    | 0.885   |
| <b>Alcohol</b>          |                     |                   |         |                       |                  |         |
| No                      | Ref                 |                   |         |                       |                  |         |
| Yes                     | -0.026              | -0.133, 0.082     | 0.641   |                       |                  |         |

Table 8 Univariate and Multivariate analysis of FMT

| Predictive factors | Univariate analysis |                 |         | Multivariate analysis |                |         |
|--------------------|---------------------|-----------------|---------|-----------------------|----------------|---------|
|                    | Beta Coefficient    | 95% CI          | p-value | Beta Coefficient      | 95% CI         | p-value |
| Age                | -0.410              | -0.801, -0.018  | 0.040   | -0.424                | -0.813, -0.034 | 0.033   |
| Sex                |                     |                 |         |                       |                |         |
| Male               | Ref                 |                 |         | Ref                   |                |         |
| Female             | -7.131              | -19.523, 5.262  | 0.259   | -7.871                | -20.039, 4.296 | 0.205   |
| Refractive error   |                     |                 |         |                       |                |         |
| Myopia             | 3.680               | -11.976, 19.337 | 0.645   |                       |                |         |
| Normal             | Ref                 |                 |         |                       |                |         |
| Hyperopia          | -4.983              | -19.483, 9.516  | 0.501   |                       |                |         |
| Smoking            |                     |                 |         |                       |                |         |
| No                 | Ref                 |                 |         |                       |                |         |
| Yes                | 15.948              | -9.522, 41.417  | 0.220   |                       |                |         |
| Alcohol            |                     |                 |         |                       |                |         |
| No                 | Ref                 |                 |         |                       |                |         |
| Yes                | 13.906              | -3.198, 31.011  | 0.111   |                       |                |         |

Table 9 Correlation between vitreous structure and age groups

| Category<br>n (%)                        | Age groups (years) |          |          | Mean Age<br>(mean±SD) |
|--|--------------------|----------|----------|-----------------------|
|  | 20-40              | 41-60    | ≥61      |                       |
| <b>Vitreous degeneration<sup>a</sup></b> |                    |          |          |                       |
| 0  | 54 (71%)           | 12 (17%) | 0        | 35.0±9.5              |
| 1  | 18 (23%)           | 35 (48%) | 5 (7%)   | 52.5±10.6             |
| 2  | 2 (3%)             | 13 (18%) | 14(19%)  | 59.8±9.1              |
| 3  | 2 (3%)             | 10 (14%) | 12 (17%) | 61.5±10.6             |
| Non-gradable <sup>b</sup>                | 0                  | 2 (2%)   | 41 (57%) | 65.9±6.5              |
| <b>PVD staging<sup>c</sup></b>           |                    |          |          |                       |
| 0  | 68 (89%)           | 17 (26%) | 1(1%)    | 33.7±10.9             |
| 1  | 6 (8%)             | 32 (47%) | 13 (18%) | 46.5±11.9             |
| 2  | 2 (3%)             | 11 (17%) | 14 (19%) | 55.8±9.6              |
| 3a                                       | 0                  | 0        | 3(4%)    | 58.2±9.6              |
| 3b                                       | 0                  | 1 (2%)   | 1 (1%)   | 57.8±8.5              |
| 4  | 0                  | 5 (8%)   | 40 (57%) | 63.3±6.8              |

<sup>a</sup> Grading of vitreous degeneration: 0 – Premacular bursa without neighboring spaces in its vicinity; 1 – Shallow neighboring spaces with no connection to the bursa; 2 – Connection to the neighboring shallow spaces; 3 – Connection between bursa and larger anterior lacuna

<sup>b</sup> Non-gradable eyes were anyone who had a previous posterior vitreous detachment

<sup>c</sup> PVD staging: stage 0 – no PVD; stage 1 – paramacular PVD; stage 2 – perifoveal PVD; stage 3a – vitreofoveal separation with persistent attachment to the optic disc and intact posterior precortical vitreous pocket; stage 3b – vitreofoveal separation with disc disrupted posterior wall of the posterior precortical vitreous pocket; stage 4 – complete PVD

Figure 9 Bar chart showing a comparison of the distribution of the vitreous degeneration grading among the 3 age groups

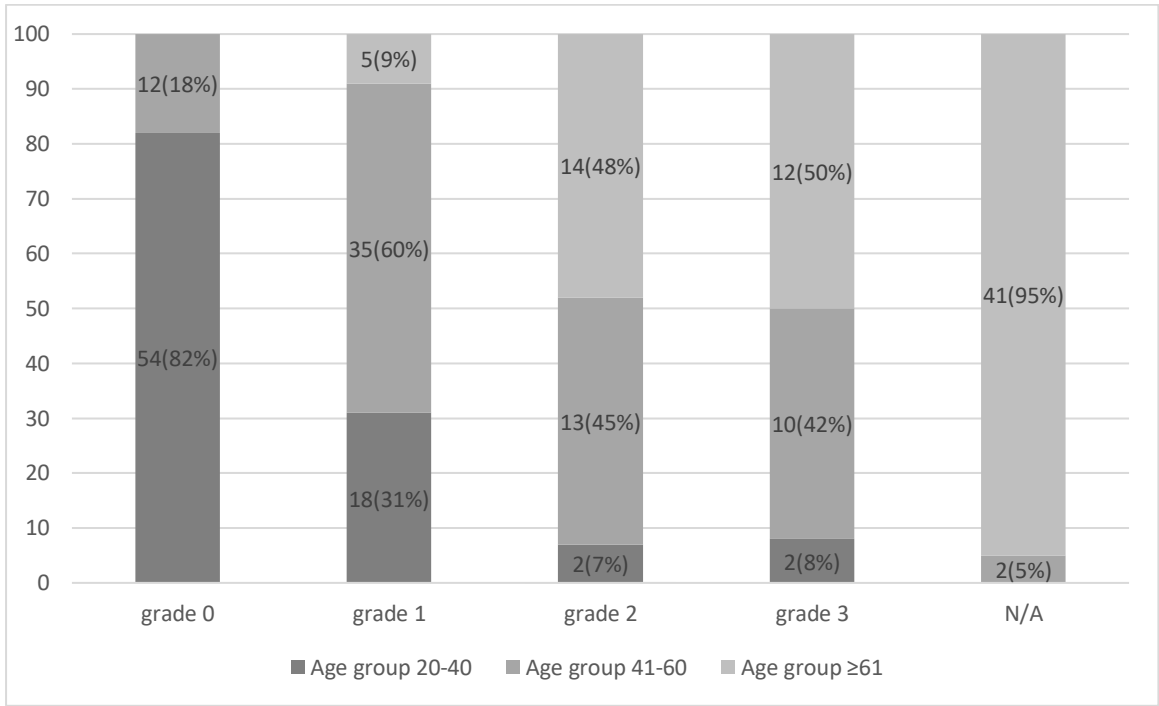


Figure 10 Bar chart showing a comparison of the distribution of the PVD staging among the 3 age groups

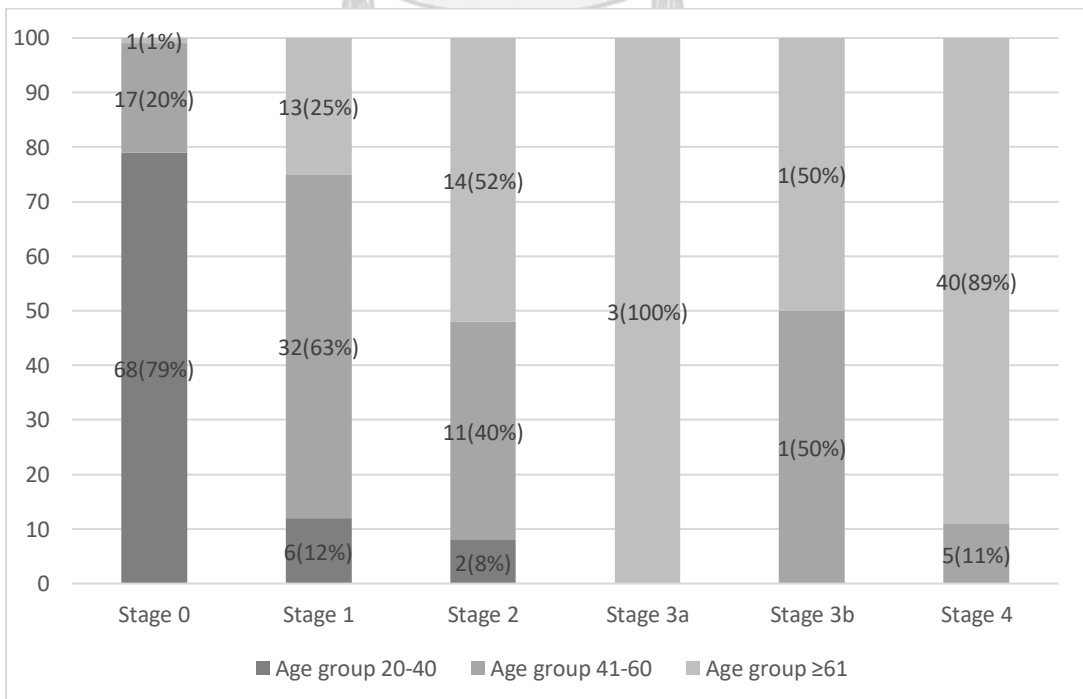


Figure 11 Bar chart showing a comparison of the distribution of the PVD staging between male and female eyes in 3 age groups

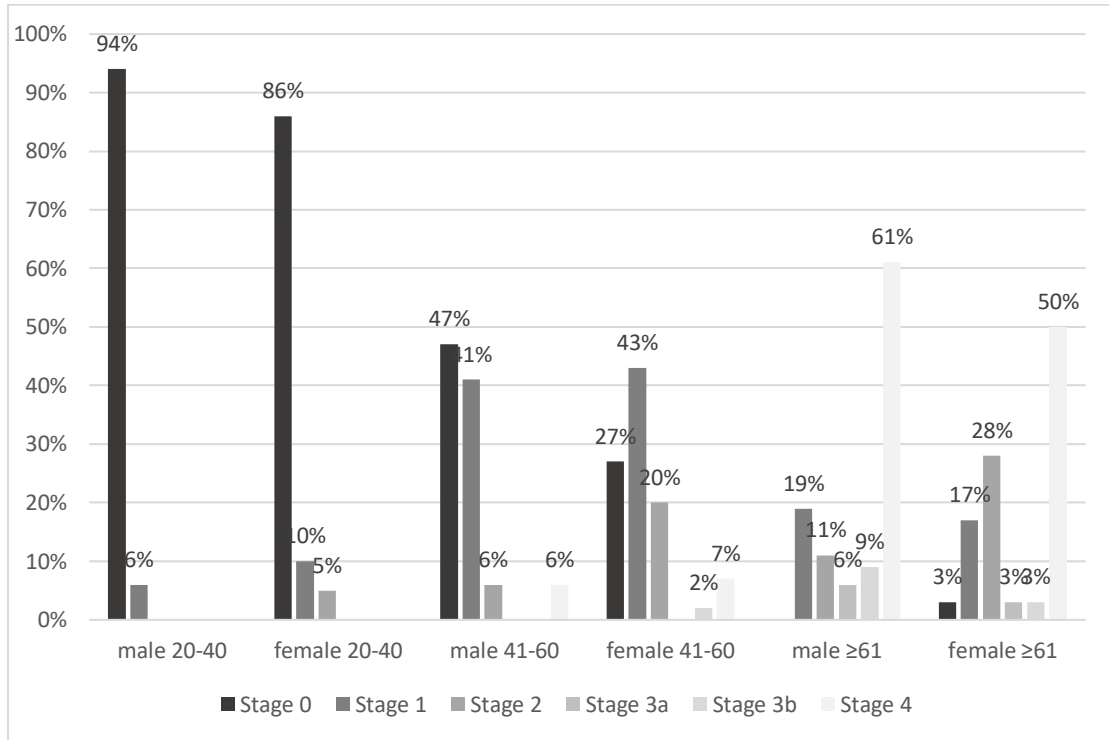


Table 10 FAZ area measured by OCTA of healthy eyes in different studies

| Authors           | Year | Subjects | Eye | Age               | SCP-FAZ<br>(mean±SD<br>, mm <sup>2</sup> ) | DCP-FAZ<br>(mean±SD<br>, mm <sup>2</sup> ) | Device                |
|-------------------|------|----------|-----|-------------------|--|--|-----------------------|
| de Carlo et al.   | 2015 | 28       | 22  | 54.0<br>±<br>11.6 | 0.288 ±<br>0.136                           |  | AngioVue<br>, Optovue |
| Kuehlewein et al. | 2015 | 19       | 13  | 31 ±<br>5         | 0.304 ±<br>0.132                           | 0.486 ±<br>0.162                           | Angioplex<br>, Cirrus |
| Samara et al.     | 2015 | 67       | 70  | 42                | 0.266 ±<br>0.097                           | 0.495 ±<br>0.227                           | AngioVue<br>, Optovue |
| Takase et al.     | 2015 | N/A      | 19  | 62.8<br>±<br>11.3 | 0.250 ±<br>0.060                           | 0.380 ±<br>0.110                           | AngioVue<br>, Optovue |
| Yu et al.         | 2015 | 45       | 76  | 36 ±<br>11        | 0.474 ±<br>0.172                           |  | AngioVue<br>, Optovue |
| Carpineto et al.  | 2016 | 60       | 60  | 28.9<br>± 7.6     | 0.251 ±<br>0.096                           |  | AngioVue<br>, Optovue |
| Coscas et al.     | 2016 | 70       | 135 | 48.3<br>±<br>17.5 | 0.280 ±<br>0.100                           | 0.370 ±<br>0.120                           | AngioVue<br>, Optovue |
| Gadde et al.      | 2016 | N/A      | 52  | 20 to<br>67       | 0.350 ±<br>0.013                           | 0.490 ±<br>0.012                           | AngioVue<br>, Optovue |



| Authors          | Year | Subjects | Eye s | Age               | SCP-FAZ<br>(mean±SD<br>, mm <sup>2</sup> ) | DCP-FAZ<br>(mean±SD<br>, mm <sup>2</sup> ) | Device                                |
|------------------|------|----------|-------|-------------------|--|--|---------------------------------------|
| Iafe et al.      | 2016 | 70       | 113   | 48 ±<br>20        | 0.289 ±<br>0.11                            | 0.614 ±<br>0.20                            | AngioVue<br>, Optovue                 |
| Linderman et al. | 2016 | 116      | 116   | 30.5<br>±<br>14.5 | 0.257 ±<br>0.104                           |  | AngioVue<br>, Optovue                 |
| Lupidi et al.    | 2016 | 47       | 47    | 39                | 0.28 ±<br>0.11                             | 0.30 ±<br>0.10                             | Spectralis<br>OCT2,<br>Heidelber<br>g |
| Magrath et al.   | 2016 | 25       | 50    | 33                | 0.274                                      | 0.364                                      | AngioVue<br>, Optovue                 |
| Shahlaee et al.  | 2016 | 17       | 34    |                   | 0.270 ±<br>0.101                           | 0.340 ±<br>0.116                           | SS-OCTA                               |
| Tan et al.       | 2016 | 117      | 117   | 22.5              | 0.240                                      | 0.380                                      | AngioVue<br>, Optovue                 |
| Wang et al.      | 2016 | 105      | 105   | 35.9<br>±<br>13.8 | 0.35 ±<br>0.12                             |  | AngioVue<br>, Optovue                 |
| Choi et al.      | 2017 | 52       | 52    | 52.1<br>±         | 0.350 ±<br>0.110                           |  | Angioplex<br>, Cirrus                 |

| Authors             | Year | Subjects | Eye<br>s | Age                    | SCP-FAZ<br>(mean±SD<br>, mm <sup>2</sup> ) | DCP-FAZ<br>(mean±SD<br>, mm <sup>2</sup> ) | Device                   |
|---------------------|------|----------|----------|------------------------|--|--|--------------------------|
|                     |      |          |          | 14.7<br>9              |  |  |                          |
| Ghassemi et al.     | 2017 | 112      | 224      | 37.0<br>±<br>11.2<br>7 | 0.27 ±<br>0.11                             | 0.35 ±<br>0.12                             | AngioVue<br>, Optovue    |
| Goudot et al.       | 2017 | 22       | 22       | 51 ±<br>17             | 0.285 ±<br>0.150                           | 0.398 ±<br>0.138                           | AngioVue<br>, Optovue    |
| Guo et al.          | 2017 | 22       | 25       | 55                     | 0.373 ±<br>0.109                           |  | Angioplex<br>, Cirrus    |
| Mastropasqua et al. | 2017 | 64       | 64       | 34.4<br>±<br>10.9      | 0.269 ±<br>0.092                           |  | DRI<br>Triton,<br>Topcon |
| Falavarjani et al.  | 2018 | 70       | 70       | 42.8<br>±<br>17.2      | 0.32 ±<br>0.11                             | 0.50 ±<br>0.13                             | AngioVue<br>, Optovue    |
| Gomez-Ulla F et al. | 2019 | 120      | 240      | 39.2<br>±<br>17.4      | 0.275 ±<br>0.106                           | 0.298 ±<br>0.108                           | DRI<br>Triton,<br>Topcon |
| Hayati et al.       | 2019 | 128      | 128      | 46                     | 0.33 ±                                     |  | RS-3000,                 |

| Authors    | Year | Subjects | Eye<br>s | Age               | SCP-FAZ<br>(mean±SD<br>, mm <sup>2</sup> ) | DCP-FAZ<br>(mean±SD<br>, mm <sup>2</sup> ) | Device               |
|------------|------|----------|----------|-------------------|--|--|----------------------|
|            |      |          |          |                   | 0.12                                       |  | Nidek                |
| This study | 2020 | 112      | 224      | 48.8<br>±<br>15.6 | 0.31 ± 0.1                                 | 0.56 ±<br>0.22                             | Plex elite,<br>Zeiss |



จุฬาลงกรณ์มหาวิทยาลัย  
CHULALONGKORN UNIVERSITY

## REFERENCES

1. Sebag J. Ageing of the vitreous. *Eye (Lond)*. 1987;1 ( Pt 2):254-62.
2. Sebag J. Anatomy and pathology of the vitreo-retinal interface. *Eye (Lond)*. 1992;6 ( Pt 6):541-52.
3. American Academy of Ophthalmology. *Retina and vitreous, 1992-1993*. San Francisco, Calif.: American Academy of Ophthalmology; 1992. 272 p. p.
4. Itakura H, Kishi S, Li D, Akiyama H. Observation of posterior precortical vitreous pocket using swept-source optical coherence tomography. *Invest Ophthalmol Vis Sci*. 2013;54(5):3102-7.
5. Schaal KB, Pang CE, Pozzoni MC, Engelbert M. The premacular bursa's shape revealed in vivo by swept-source optical coherence tomography. *Ophthalmology*. 2014;121(5):1020-8.
6. Duker JS, Kaiser PK, Binder S, de Smet MD, Gaudric A, Reichel E, et al. The International Vitreomacular Traction Study Group classification of vitreomacular adhesion, traction, and macular hole. *Ophthalmology*. 2013;120(12):2611-9.
7. Sebag J. Anomalous posterior vitreous detachment: a unifying concept in vitreo-retinal disease. *Graefes Arch Clin Exp Ophthalmol*. 2004;42(8):690-8.
8. Jonas JB, Schneider U, Naumann GO. Count and density of human retinal photoreceptors. *Graefes Arch Clin Exp Ophthalmol*. 1992;30(6):505-10.
9. Takase N, Nozaki M, Kato A, Ozeki H, Yoshida M, Ogura Y. Enlargement of Foveal Avascular Zone in Diabetic Eyes Evaluated by En Face Optical Coherence Tomography Angiography. *Retina*. 2015;35(11):2377-83.
10. Freiberg FJ, Pfau M, Wons J, Wirth MA, Becker MD, Michels S. Optical coherence tomography angiography of the foveal avascular zone in diabetic retinopathy. *Graefes Arch Clin Exp Ophthalmol*. 2016;254(6):1051-8.
11. Hayreh SS. Blood supply of the optic nerve head. *Ophthalmologica*. 1996;210(5):285-95.
12. Hayreh SS. The blood supply of the optic nerve head and the evaluation of it - myth and reality. *Prog Retin Eye Res*. 2001;20(5):563-93.
13. Michaelson IC, Herz N, Lewkowitz E, Kertesz D. Effect of increased oxygen on

the development of the retinal vessels; an experimental study. *Br J Ophthalmol.* 1954;38(10):577-87.

14. Henkind P. Radial peripapillary capillaries of the retina. I. Anatomy: human and comparative. *Br J Ophthalmol.* 1967;51(2):115-23.

15. Chui TY, VanNasdale DA, Elsner AE, Burns SA. The association between the foveal avascular zone and retinal thickness. *Invest Ophthalmol Vis Sci.* 2014;55(10):6870-7.

16. Wojtkowski M, Bajraszewski T, Gorczynska I, Targowski P, Kowalczyk A, Wasilewski W, et al. Ophthalmic imaging by spectral optical coherence tomography. *Am J Ophthalmol.* 2004;138(3):412-9.

17. Leitgeb R, Hitzinger C, Fercher A. Performance of fourier domain vs. time domain optical coherence tomography. *Opt Express.* 2003;11(8):889-94.

18. Spaide RF, Fujimoto JG, Waheed NK, Sadda SR, Staurengi G. Optical coherence tomography angiography. *Prog Retin Eye Res.* 2018;64:1-55.

19. Jia Y, Morrison JC, Tokayer J, Tan O, Lombardi L, Baumann B, et al. Quantitative OCT angiography of optic nerve head blood flow. *Biomed Opt Express.* 2012;3(12):3127-37.

20. Leveque PM, Zeboulon P, Brasnu E, Baudouin C, Labbe A. Optic Disc Vascularization in Glaucoma: Value of Spectral-Domain Optical Coherence Tomography Angiography. *J Ophthalmol.* 2016;2016:6956717.

21. Chen CL, Bojikian KD, Gupta D, Wen JC, Zhang Q, Xin C, et al. Optic nerve head perfusion in normal eyes and eyes with glaucoma using optical coherence tomography-based microangiography. *Quant Imaging Med Surg.* 2016;6(2):125-33.

22. Spaide RF, Curcio CA. Evaluation of Segmentation of the Superficial and Deep Vascular Layers of the Retina by Optical Coherence Tomography Angiography Instruments in Normal Eyes. *JAMA Ophthalmol.* 2017;135(3):259-62.

23. Savastano MC, Lumbroso B, Rispoli M. In Vivo Characterization of Retinal Vascularization Morphology Using Optical Coherence Tomography Angiography. *Retina.* 2015;35(11):2196-203.

24. Wylegata A, Wang L, Zhang S, Liu Z, Teper S, Wylegata E. Comparison of foveal

avascular zone and retinal vascular density in healthy Chinese and Caucasian adults. *Acta Ophthalmologica*. 2020;98(4):e464-e9.

25. Falavarjani KG, Shenazandi H, Naseri D, Anvari P, Kazemi P, Aghamohammadi F, et al. Foveal avascular zone and vessel density in healthy subjects: an optical coherence tomography angiography study. *Journal of ophthalmic & vision research*. 2018;13(3):260.
26. Tan CS, Lim LW, Chow VS, Chay IW, Tan S, Cheong KX, et al. Optical Coherence Tomography Angiography Evaluation of the Parafoveal Vasculature and Its Relationship With Ocular Factors. *Invest Ophthalmol Vis Sci*. 2016;57(9):OCT224-34.
27. Kuehlewein L, Tepelus TC, An L, Durbin MK, Srinivas S, Sadda SR. Noninvasive Visualization and Analysis of the Human Parafoveal Capillary Network Using Swept Source OCT Optical Microangiography. *Invest Ophthalmol Vis Sci*. 2015;56(6):3984-8.
28. Fujiwara A, Morizane Y, Hosokawa M, Kimura S, Shiode Y, Hirano M, et al. Factors affecting foveal avascular zone in healthy eyes: An examination using swept-source optical coherence tomography angiography. *Plos one*. 2017;12(11):e0188572.
29. Kim YC, Harasawa M, Salcedo-Villanueva G, Siringo FS, Paciuc-Beja M, Olson JL, et al. Enhanced High-Density Line Spectral-Domain Optical Coherence Tomography Imaging of the Vitreoretinal Interface: Description of Selected Cases. *Semin Ophthalmol*. 2016;31(6):559-66.
30. Itakura H, Kishi S, Li D, Akiyama H. En face imaging of posterior precortical vitreous pockets using swept-source optical coherence tomography. *Invest Ophthalmol Vis Sci*. 2015;56(5):2898-900.
31. Park JW, Lee JE, Pak KY. Posterior Vitreous Structures Evaluated by Swept-source Optical Coherence Tomography with En Face Imaging. *Korean J Ophthalmol*. 2018;32(5):376-81.
32. Rao HL, Pradhan ZS, Weinreb RN, Reddy HB, Riyazuddin M, Sachdeva S, et al. Determinants of peripapillary and macular vessel densities measured by optical coherence tomography angiography in normal eyes. *Journal of glaucoma*. 2017;26(5):491-7.
33. Khodabandeh A, Shahraki K, Roohipour R, Riazi-Esfahani H, Yaseri M, Faghihi H, et al. Quantitative measurement of vascular density and flow using optical coherence

tomography angiography (OCTA) in patients with central retinal vein occlusion: Can OCTA help in distinguishing ischemic from non-ischemic type? *Int J Retina Vitreous*. 2018;4:47.

34. Fernandez-Vigo JI, Kudsieh B, Shi H, De-Pablo-Gomez-de-Liano L, Serrano-Garcia I, Ruiz-Moreno JM, et al. Normative Database of Peripapillary Vessel Density Measured by Optical Coherence Tomography Angiography and Correlation Study. *Curr Eye Res*. 2020:1-8.

35. Mase T, Ishibazawa A, Nagaoka T, Yokota H, Yoshida A. Radial peripapillary capillary network visualized using wide-field montage optical coherence tomography angiography. *Investigative ophthalmology & visual science*. 2016;57(9):OCT504-OCT10.

36. Paula KY, Cringle SJ, Yu D-Y. Correlation between the radial peripapillary capillaries and the retinal nerve fibre layer in the normal human retina. *Experimental eye research*. 2014;129:83-92.

37. Hou H, Moghimi S, Zangwill LM, Shoji T, Ghahari E, Manalastas PIC, et al. Inter-eye Asymmetry of Optical Coherence Tomography Angiography Vessel Density in Bilateral Glaucoma, Glaucoma Suspect, and Healthy Eyes. *Am J Ophthalmol*. 2018;190:69-77.

38. Werner AC, Shen LQ. A Review of OCT Angiography in Glaucoma. *Semin Ophthalmol*. 2019;34(4):279-86.

39. Samara WA, Say EA, Khoo CT, Higgins TP, Magrath G, Ferenczy S, et al. Correlation of Foveal Avascular Zone Size with Foveal Morphology in Normal Eyes Using Optical Coherence Tomography Angiography. *Retina*. 2015;35(11):2188-95.

40. Laatikainen L, Larinkari J. Capillary-free area of the fovea with advancing age. *Investigative Ophthalmology & Visual Science*. 1977;16(12):1154-7.

41. Mammo Z, Balaratnasingam C, Yu P, Xu J, Heisler M, Mackenzie P, et al. Quantitative noninvasive angiography of the fovea centralis using speckle variance optical coherence tomography. *Investigative ophthalmology & visual science*. 2015;56(9):5074-86.

42. Carpineto P, Mastropasqua R, Marchini G, Toto L, Di Nicola M, Di Antonio L. Reproducibility and repeatability of foveal avascular zone measurements in healthy subjects by optical coherence tomography angiography. *Br J Ophthalmol*.

2016;100(5):671-6.

43. Choi J, Kwon J, Shin JW, Lee J, Lee S, Kook MS. Quantitative optical coherence tomography angiography of macular vascular structure and foveal avascular zone in glaucoma. *PLoS One*. 2017;12(9):e0184948.
44. Coscas F, Sellam A, Glacet-Bernard A, Jung C, Goudot M, Miere A, et al. Normative Data for Vascular Density in Superficial and Deep Capillary Plexuses of Healthy Adults Assessed by Optical Coherence Tomography Angiography. *Invest Ophthalmol Vis Sci*. 2016;57(9):OCT211-23.
45. de Carlo TE, Chin AT, Bonini Filho MA, Adhi M, Branchini L, Salz DA, et al. Detection of Microvascular Changes in Eyes of Patients with Diabetes but Not Clinical Diabetic Retinopathy Using Optical Coherence Tomography Angiography. *Retina*. 2015;35(11):2364-70.
46. Gadde SG, Anegondi N, Bhanushali D, Chidambara L, Yadav NK, Khurana A, et al. Quantification of Vessel Density in Retinal Optical Coherence Tomography Angiography Images Using Local Fractal Dimension. *Invest Ophthalmol Vis Sci*. 2016;57(1):246-52.
47. Guo J, She X, Liu X, Sun X. Repeatability and Reproducibility of Foveal Avascular Zone Area Measurements Using AngioPlex Spectral Domain Optical Coherence Tomography Angiography in Healthy Subjects. *Ophthalmologica*. 2017;237(1):21-8.
48. Goudot MM, Sikorav A, Semoun O, Miere A, Jung C, Courbebaisse B, et al. Parafoveal OCT Angiography Features in Diabetic Patients without Clinical Diabetic Retinopathy: A Qualitative and Quantitative Analysis. *J Ophthalmol*. 2017;2017:8676091.
49. Linderman R, Salmon AE, Strampe M, Russillo M, Khan J, Carroll J. Assessing the Accuracy of Foveal Avascular Zone Measurements Using Optical Coherence Tomography Angiography: Segmentation and Scaling. *Transl Vis Sci Technol*. 2017;6(3):16.
50. Magrath GN, Say EAT, Sioufi K, Ferenczy S, Samara WA, Shields CL. Variability in Foveal Avascular Zone and Capillary Density Using Optical Coherence Tomography Angiography Machines in Healthy Eyes. *Retina*. 2017;37(11):2102-11.
51. Mastropasqua R, Toto L, Mattei PA, Di Nicola M, Zecca IAL, Carpineto P, et al. Reproducibility and repeatability of foveal avascular zone area measurements using swept-source optical coherence tomography angiography in healthy subjects. *Eur J*



Ophthalmol. 2017;27(3):336-41.

52. Shahlæe A, Pefkianaki M, Hsu J, Ho AC. Measurement of Foveal Avascular Zone Dimensions and its Reliability in Healthy Eyes Using Optical Coherence Tomography Angiography. *Am J Ophthalmol.* 2016;161:50-5 e1.

53. Yu J, Jiang C, Wang X, Zhu L, Gu R, Xu H, et al. Macular perfusion in healthy Chinese: an optical coherence tomography angiogram study. *Invest Ophthalmol Vis Sci.* 2015;56(5):3212-7.

54. Ghassemi F, Mirshahi R, Bazvand F, Fadakar K, Faghihi H, Sabour S. The quantitative measurements of foveal avascular zone using optical coherence tomography angiography in normal volunteers. *J Curr Ophthalmol.* 2017;29(4):293-9.

55. Gomez-Ulla F, Cutrin P, Santos P, Fernandez M, Abalades M, Abalo-Lojo JM, et al. Age and gender influence on foveal avascular zone in healthy eyes. *Exp Eye Res.* 2019;189:107856.

56. Falavarjani KG, Shenazandi H, Naseri D, Anvari P, Kazemi P, Aghamohammadi F, et al. Foveal Avascular Zone and Vessel Density in Healthy Subjects: An Optical Coherence Tomography Angiography Study. *J Ophthalmic Vis Res.* 2018;13(3):260-5.

57. Alnawaiseh M, Lahme L, Muller V, Rosentreter A, Eter N. Correlation of flow density, as measured using optical coherence tomography angiography, with structural and functional parameters in glaucoma patients. *Graefes Arch Clin Exp Ophthalmol.* 2018;256(3):589-97.

58. Wang Q, Chan S, Yang JY, You B, Wang YX, Jonas JB, et al. Vascular Density in Retina and Choriocapillaris as Measured by Optical Coherence Tomography Angiography. *Am J Ophthalmol.* 2016;168:95-109.

59. Wu LZ, Huang ZS, Wu DZ, Chan E. Characteristics of the macular microvasculature. *Jpn J Ophthalmol.* 1985;29(4):412-6.

60. Song WK, Lee SC, Lee ES, Kim CY, Kim SS. Macular thickness variations with sex, age, and axial length in healthy subjects: a spectral domain-optical coherence tomography study. *Invest Ophthalmol Vis Sci.* 2010;51(8):3913-8.

61. Adhi M, Aziz S, Muhammad K, Adhi MI. Macular thickness by age and gender in healthy eyes using spectral domain optical coherence tomography. *PLoS One.* 2012;7(5):e37638.

62. Sull AC, Vuong LN, Price LL, Srinivasan VJ, Gorczynska I, Fujimoto JG, et al. Comparison of spectral/Fourier domain optical coherence tomography instruments for assessment of normal macular thickness. *Retina*. 2010;30(2):235-45.
63. Ghassemi F, Fadakar K, Bazvand F, Mirshahi R, Mohebbi M, Sabour S. The Quantitative Measurements of Vascular Density and Flow Areas of Macula Using Optical Coherence Tomography Angiography in Normal Volunteers. *Ophthalmic Surg Lasers Imaging Retina*. 2017;48(6):478-86.
64. Chuo JY, Lee TY, Hollands H, Morris AH, Reyes RC, Rossiter JD, et al. Risk factors for posterior vitreous detachment: a case-control study. *Am J Ophthalmol*. 2006;142(6):931-7.
65. Shen Z, Duan X, Wang F, Wang N, Peng Y, Liu DT, et al. Prevalence and risk factors of posterior vitreous detachment in a Chinese adult population: the Handan eye study. *BMC Ophthalmol*. 2013;13(1):33.
66. Schwab C, Ivastinovic D, Borkenstein A, Lackner EM, Wedrich A, Velikay-Parel M. Prevalence of early and late stages of physiologic PVD in emmetropic elderly population. *Acta Ophthalmol*. 2012;90(3):e179-84.
67. Hayashi K, Sato T, Manabe SI, Hirata A. Sex-Related Differences in the Progression of Posterior Vitreous Detachment with Age. *Ophthalmol Retina*. 2019;3(3):237-43.
68. Gaudric A, Haouchine B, Massin P, Paques M, Blain P, Erginay A. Macular hole formation: new data provided by optical coherence tomography. *Arch Ophthalmol*. 1999;117(6):744-51.
69. Kishi S, Takahashi H. Three-dimensional observations of developing macular holes. *Am J Ophthalmol*. 2000;130(1):65-75.
70. Azzolini C, Patelli F, Brancato R. Correlation between optical coherence tomography data and biomicroscopic interpretation of idiopathic macular hole. *Am J Ophthalmol*. 2001;132(3):348-55.
71. Johnson MW, Van Newkirk MR, Meyer KA. Perifoveal vitreous detachment is the primary pathogenic event in idiopathic macular hole formation. *Arch Ophthalmol*. 2001;119(2):215-22.
72. Risk factors for idiopathic macular holes. The Eye Disease Case-Control Study

Group. Am J Ophthalmol. 1994;118(6):754-61.

73. Evans JR, Schwartz SD, McHugh JD, Thamby-Rajah Y, Hodgson SA, Wormald RP, et al. Systemic risk factors for idiopathic macular holes: a case-control study. Eye (Lond). 1998;12 ( Pt 2):256-9.

74. Kang HK, Chang AA, Beaumont PE. The macular hole: report of an Australian surgical series and meta-analysis of the literature. Clin Exp Ophthalmol. 2000;28(4):298-308.

75. Chang E, Garg P, Capone A, Jr. Outcomes and predictive factors in bilateral macular holes. Ophthalmology. 2013;120(9):1814-9.

76. Kakehashi A, Takezawa M, Akiba J. Classification of posterior vitreous detachment. Clin Ophthalmol. 2014;8:1-10.





จุฬาลงกรณ์มหาวิทยาลัย  
**CHULALONGKORN UNIVERSITY**

## VITA

**NAME** Sittikorn Laojaroenwanit

**DATE OF BIRTH** 02 June 1984

**PLACE OF BIRTH** Sisaket, Thailand

**HOME ADDRESS** 141 Mo 14 Khunhan Sisaket 33150

**PUBLICATION** Laojaroenwanit S, Layanun V, Praneeprachachon P, Pukrushpan P. Time of maximum cycloplegia after instillation of cyclopentolate 1% in children with brown irises. *Clinical Ophthalmology* (Auckland, NZ) 2016;10:897-902. doi:10.2147/OPHTH.S102611.



จุฬาลงกรณ์มหาวิทยาลัย  
CHULALONGKORN UNIVERSITY